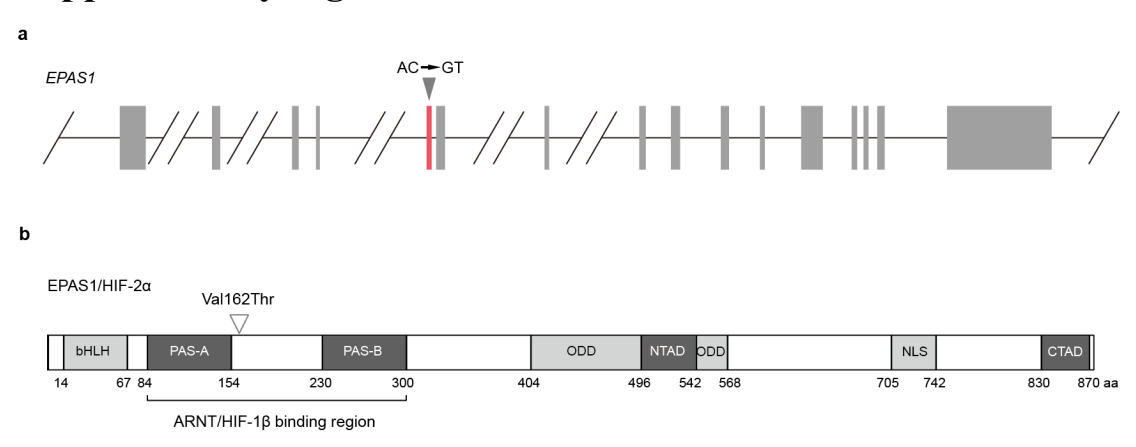
- 1 Supplementary information for:
- 2 Homeostasis of glucose and lipid metabolism during physiological responses to a
- 3 simulated hypoxic high altitude environment

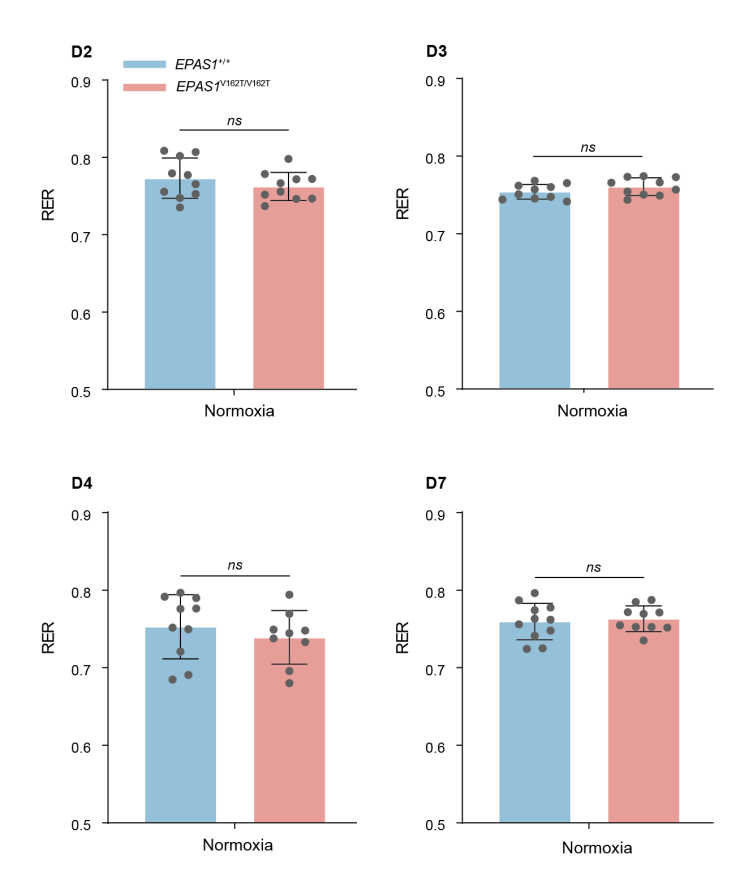
5

6

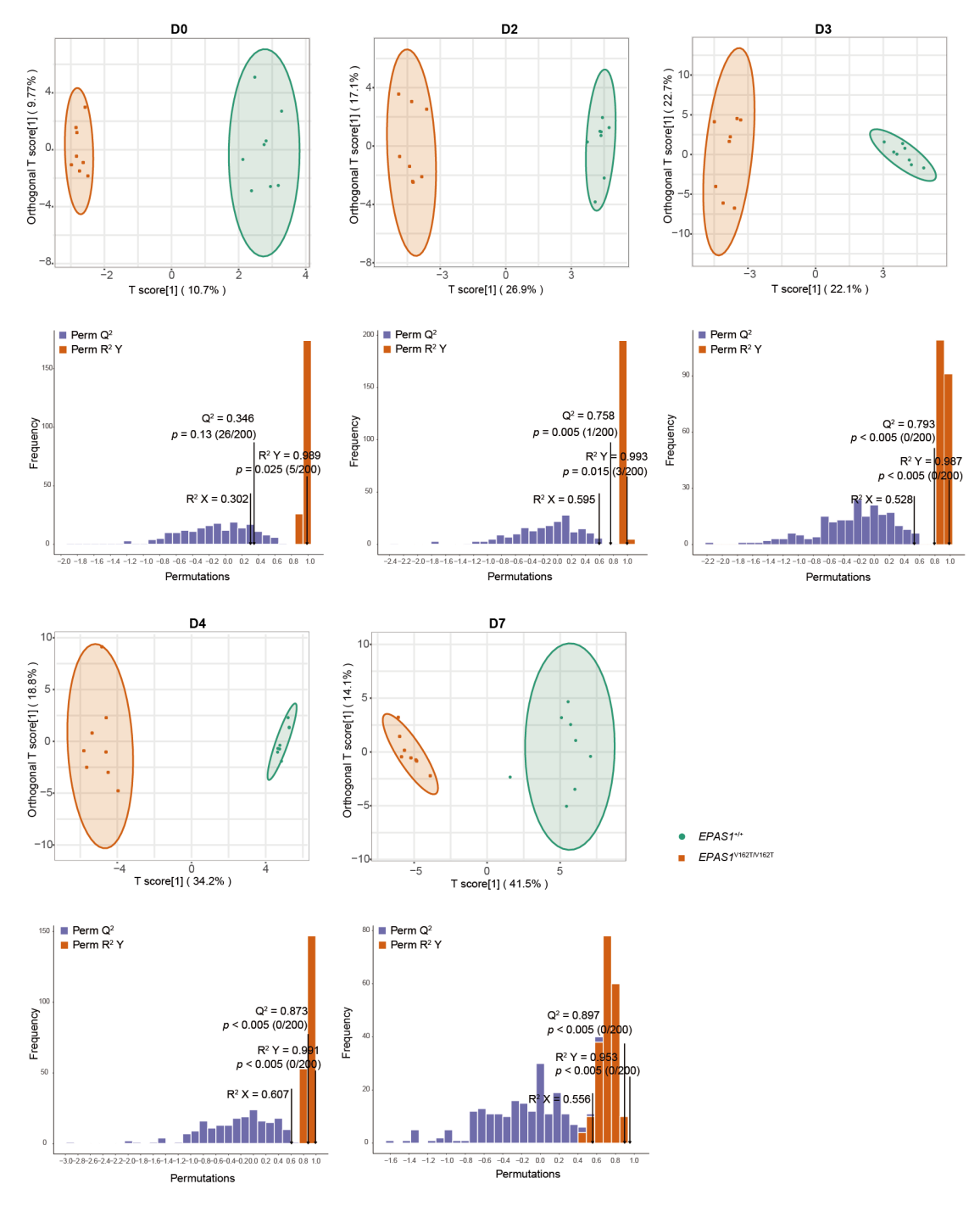
Supplementary Figures



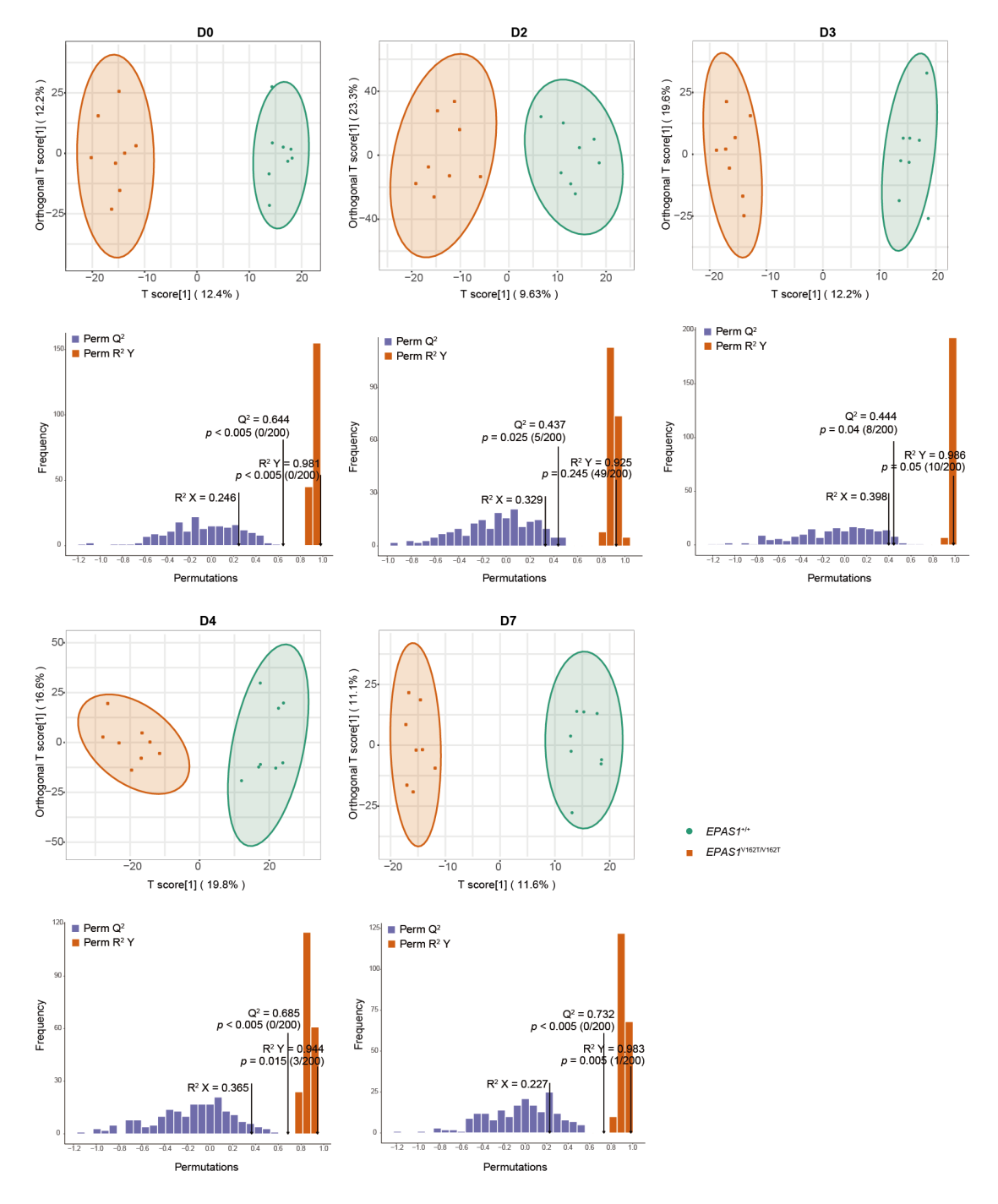
- 7 **Supplementary Fig. 1** Generation of falconized mice by editing AC into GT in Exon
- 8 5 of the *EPAS1* gene on Chromosome 17. **a**, The gene structure: exon (grey boxes),
- 9 introns (horizontal lines), the mutation site (red). **b**, The resultant amino acid
- substitution from Valine (Val) to Threonine (Thr) at the 162th residual (white triangle)
- of EPAS1 protein, bHLH: basic helix-loop-helix, PAS-A/B: per-ARNT-Sim-A/B,
- 12 ODD: oxygen-dependent degradation domain, N/CTAD: N/C-terminal transactivation
- domain, NLS: nuclear localization signal.



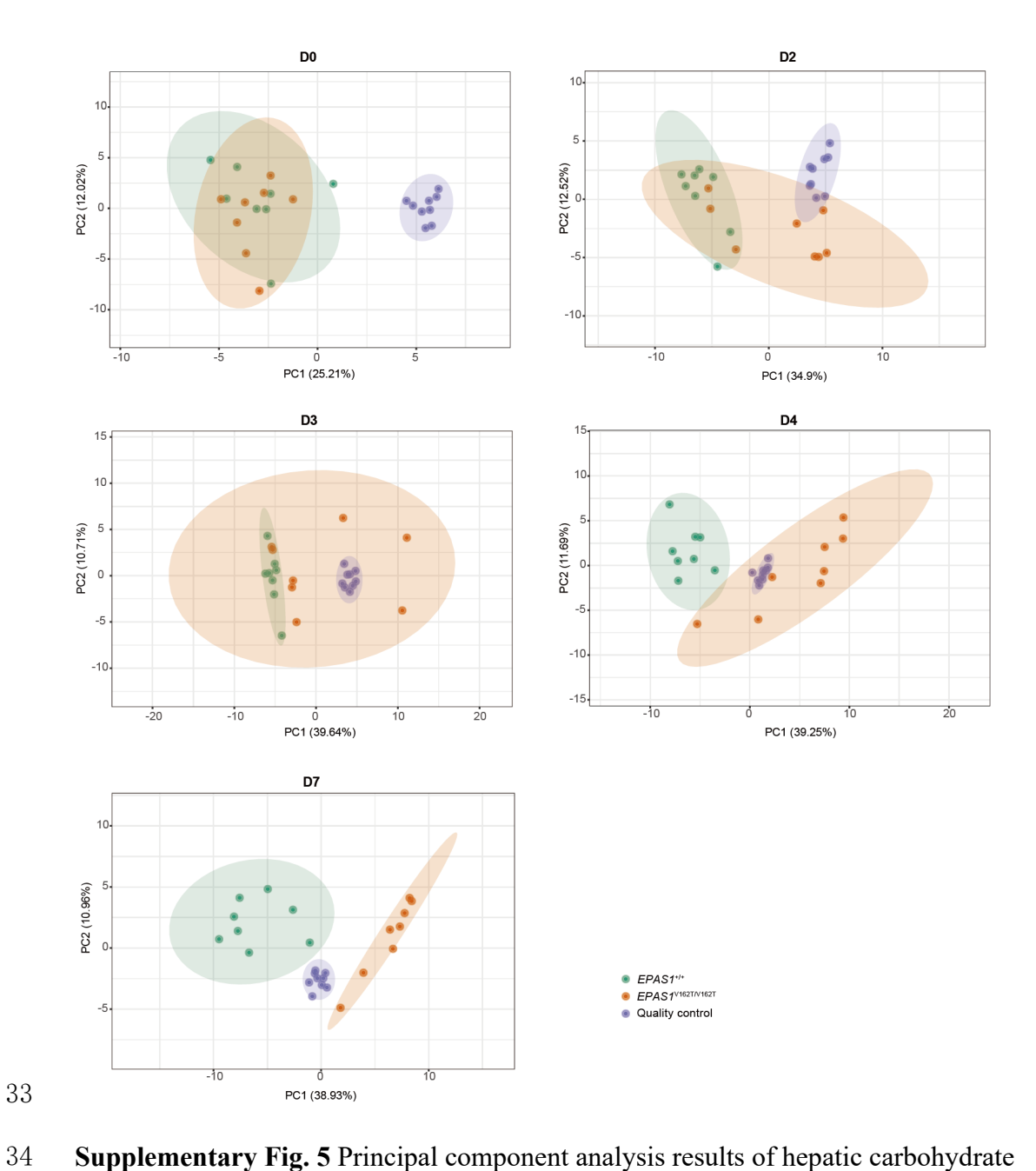
Supplementary Fig. 2 Comparison of respiratory exchange ratio (RER) values between $EPASI^{V162T/V162T}$ and $EPASI^{+/+}$ mouse individuals ($n = 10 \ vs \ 10 \ on \ D2$ and D3; 9 $vs \ 10 \ on \ D4$; 10 $vs \ 11 \ on \ D7$) under normoxia. Two-sided t tests were applied for all the comparisons. The bars display mean \pm SD. ns: no significant difference. P values for each group were 0.3035, 0.1854, 0.4500 and 0.6967. Source data are provided as a **Source Data** file.



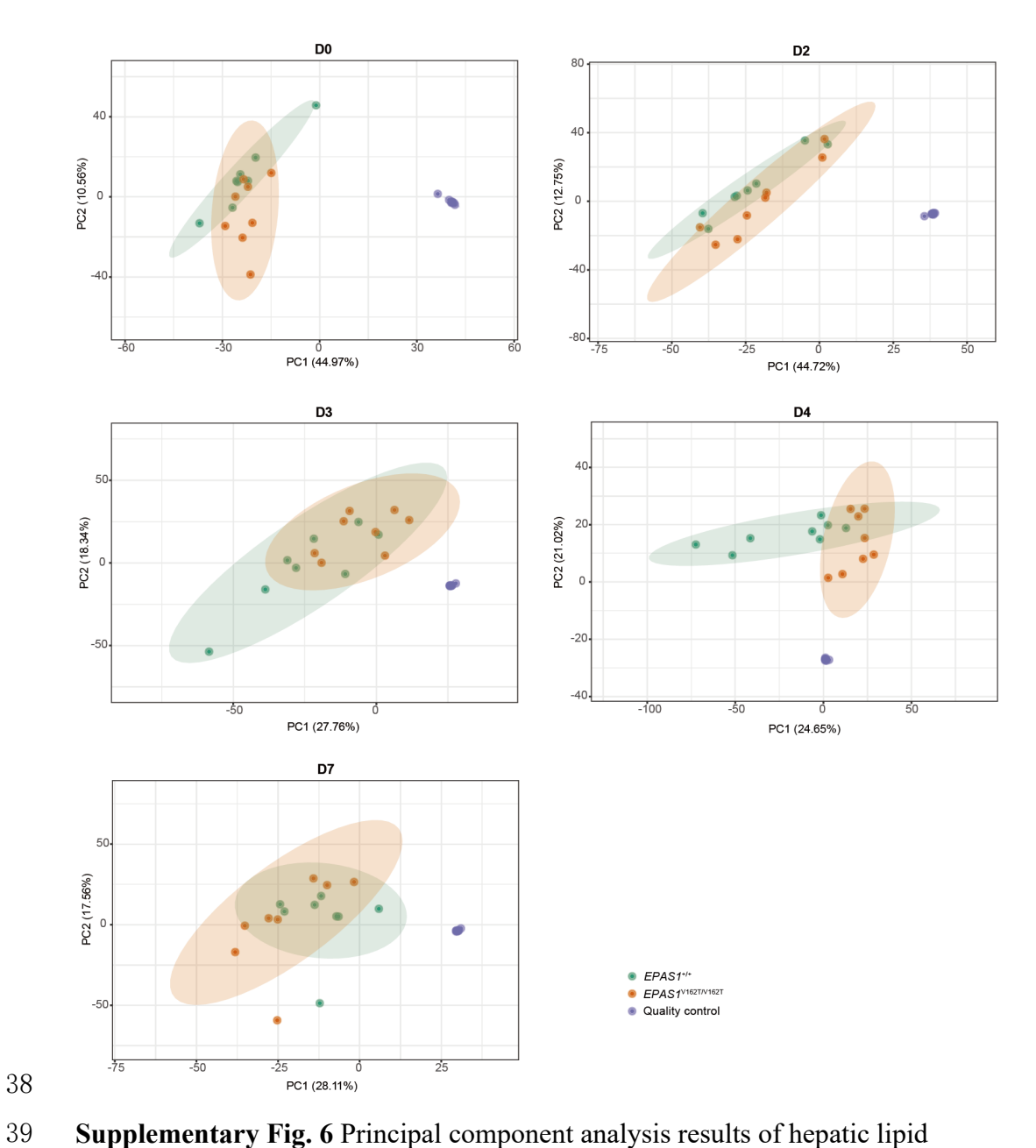
Supplementary Fig. 3 Orthogonal partial least squares-discriminant analysis results of carbohydrate metabolites in hepatic samples collected at each time point between $EPASI^{V162T/V162T}$ and $EPASI^{+/+}$ mouse individuals (n = 8 for each group on D0-D7). The x-axis represents the model's accuracy and the y-axis indicates the frequency of classification effects within the model.



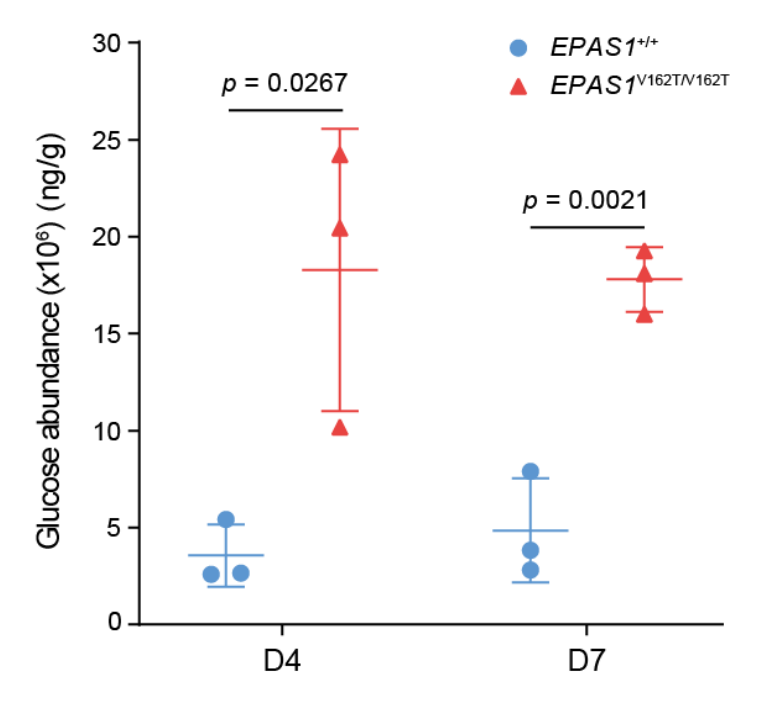
Supplementary Fig. 4 Orthogonal partial least squares-discriminant analysis results of lipid metabolites in hepatic samples collected at each time point between $EPASI^{V162T/V162T}$ and $EPASI^{+/+}$ mouse individuals (n=8 for each group on D0-D7). The x-axis represents the model's accuracy and the y-axis indicates the frequency of classification effects within the model.



Supplementary Fig. 5 Principal component analysis results of hepatic carbohydrate metabolites collected at each time point in $EPASI^{V162T/V162T}$, $EPASI^{+/+}$ mouse individuals (n = 8 for each group on D0-D7) and quality control samples (n = 9 on D0-D7).



Supplementary Fig. 6 Principal component analysis results of hepatic lipid metabolites collected at each time point in $EPAS1^{V162T/V162T}$, $EPAS1^{+/+}$ mouse individuals (n = 8 for each group on D0-D7) and quality control samples (n = 9 on D0-D7).

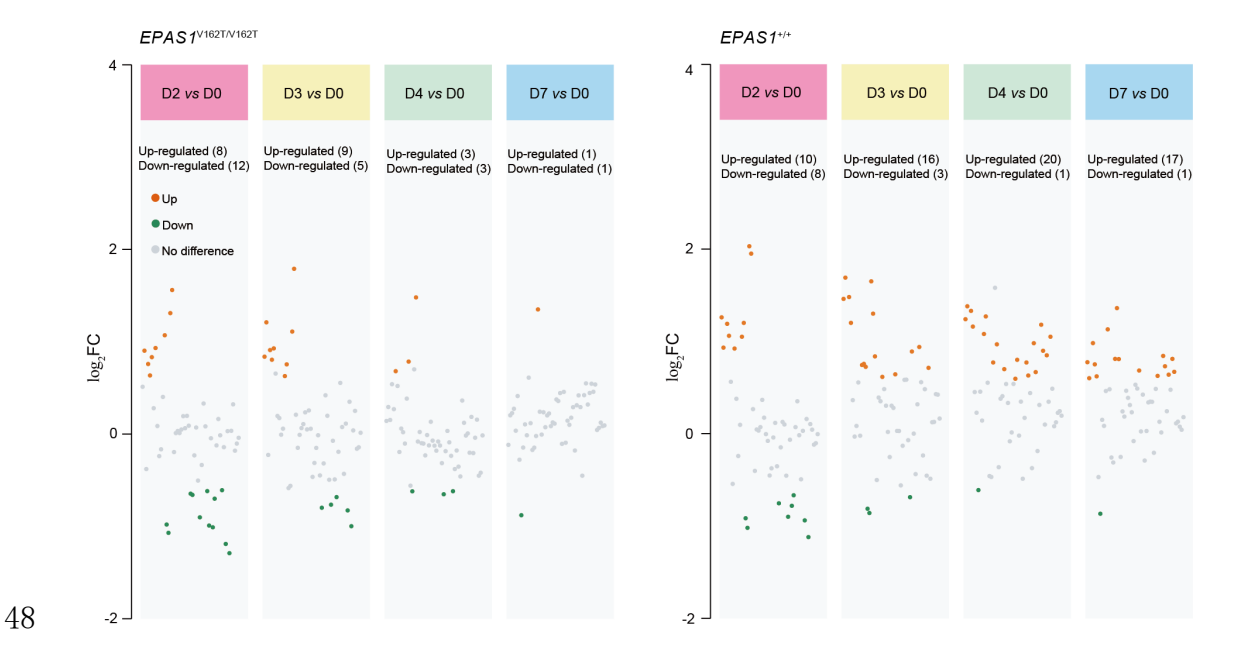


Supplementary Fig. 7 Comparisons of hepatic glucose content between

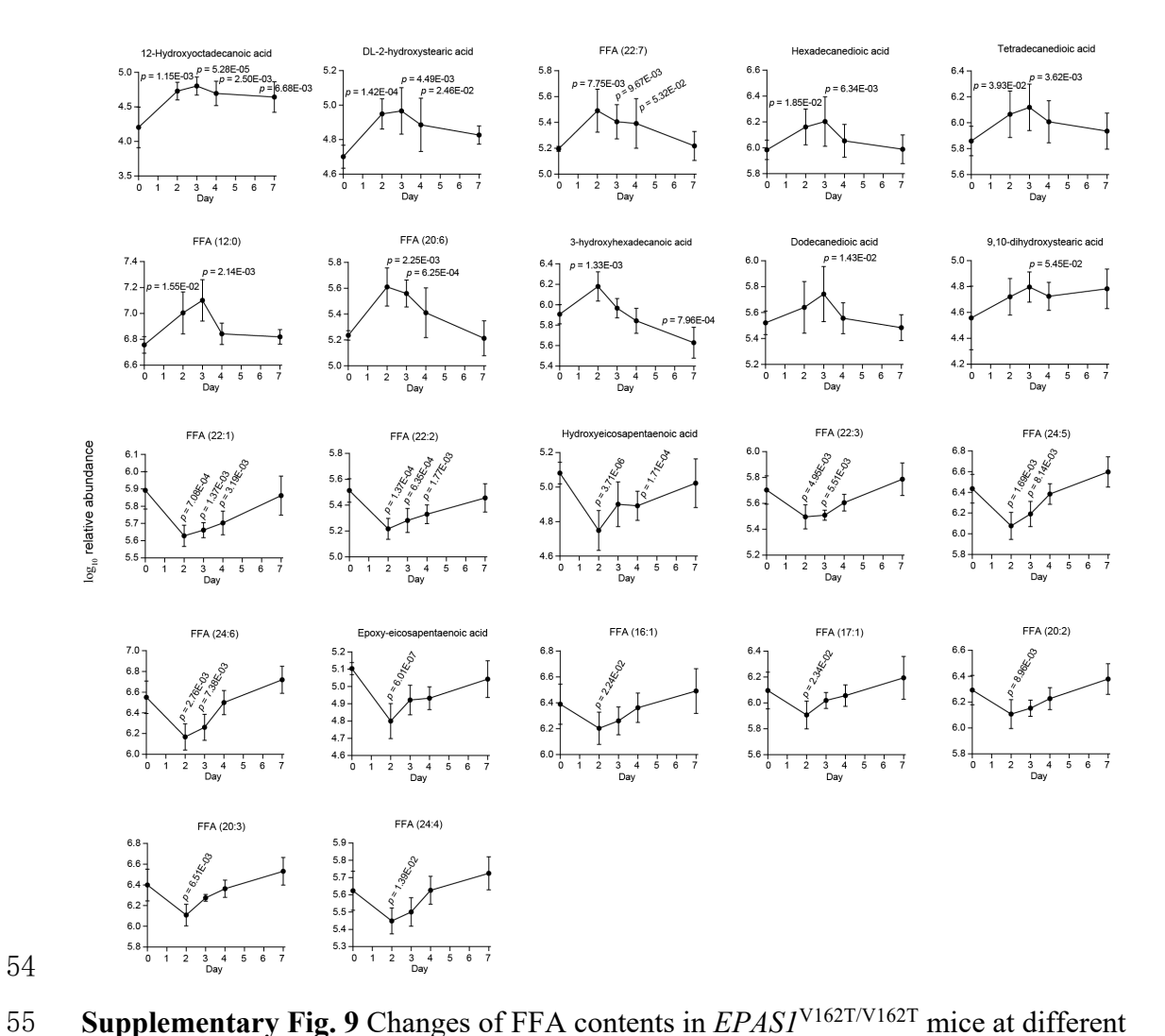
 $EPASI^{V162T/V162T}$ and $EPASI^{+/+}$ mouse individuals on D4 and D7 (n = 3 for each

group) detected using targeted metabolomics in hepatic samples. The bars show mean

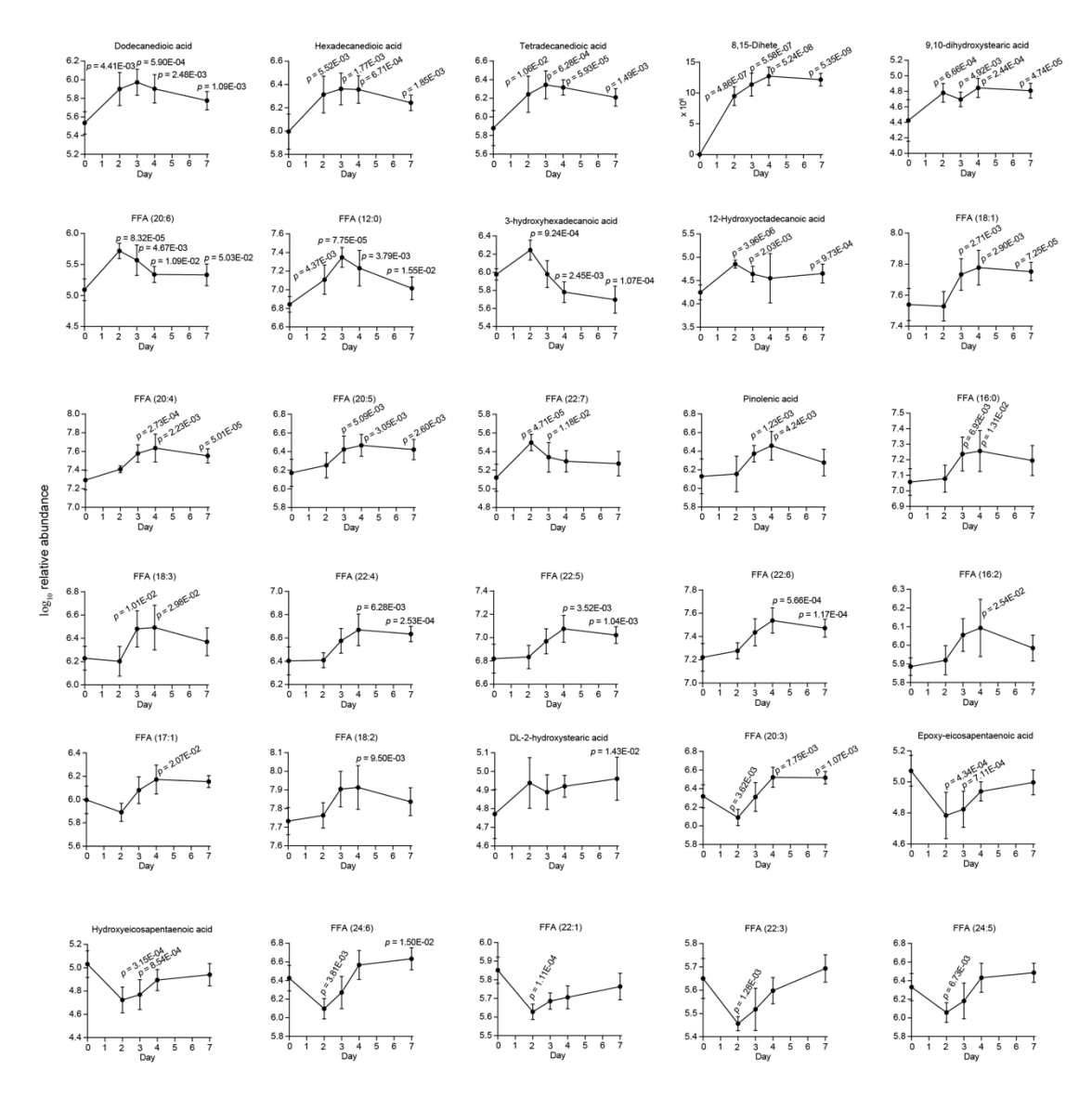
 \pm SD. Two-sided t tests were applied. Source data are provided as a **Source Data** file.



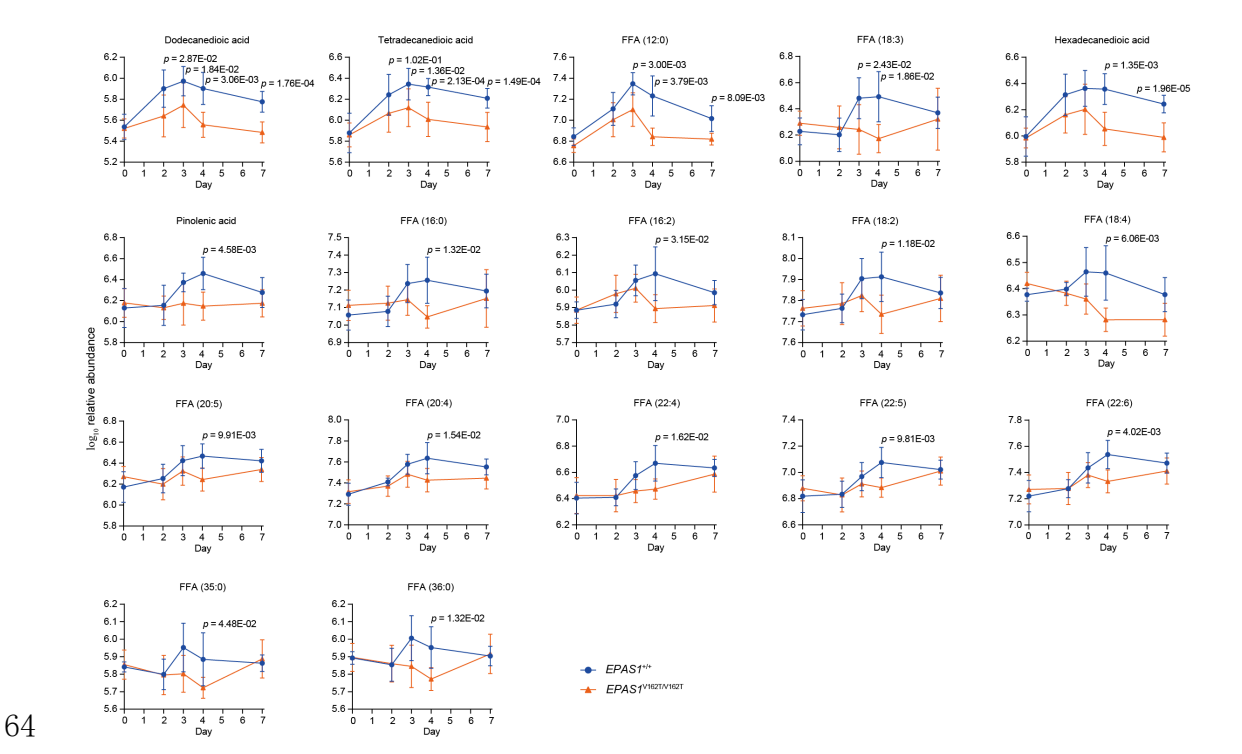
Supplementary Fig. 8 Volcano plots of differentially expressed free fatty acid (FFA) in the hepatic samples of mutant and wild type mice at each treatment interval in comparison with D0, respectively. The x-axis is the fold change (log₂FC), and y-axis is the variable important in projection (VIP). A significant difference was determined based on VIP \geq 1, and FC \geq 1.5 or FC \leq 0.67.



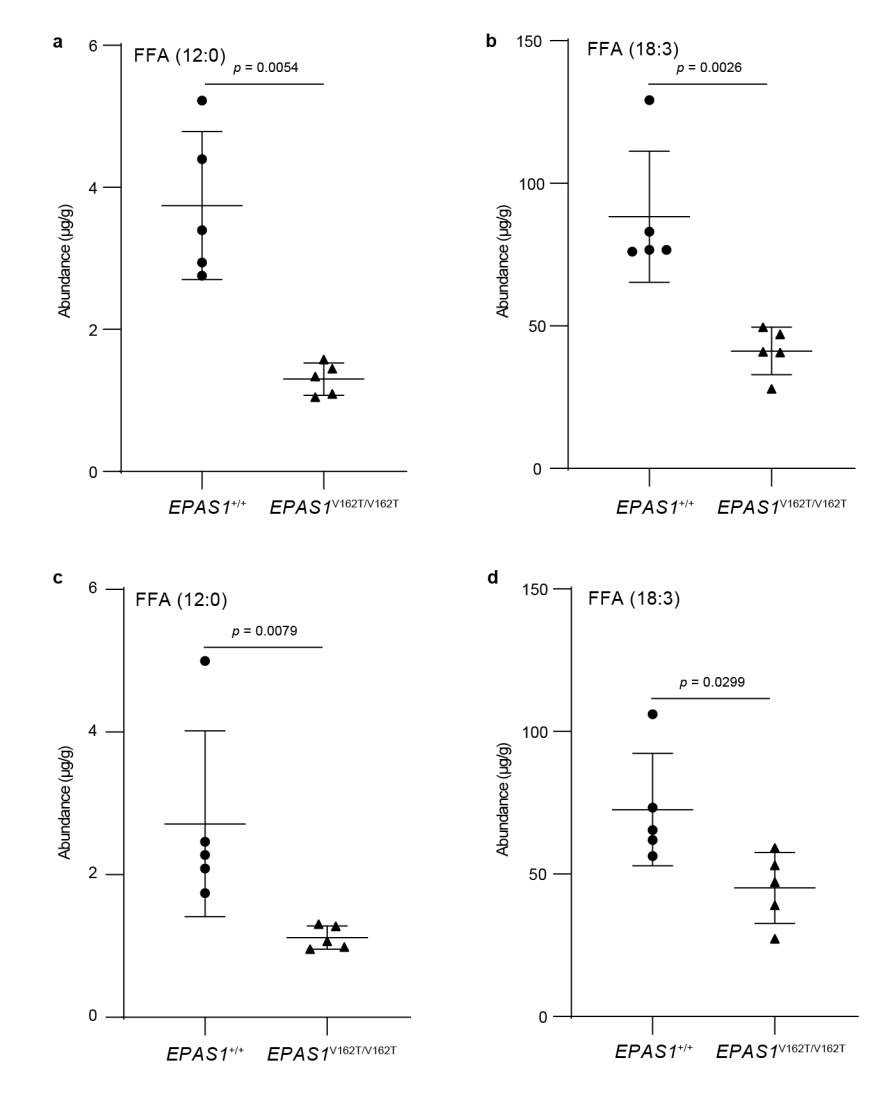
Supplementary Fig. 9 Changes of FFA contents in $EPASI^{V162T/V162T}$ mice at different time points in comparison with D0. A significant difference was determined based on $VIP \ge 1$, and $FC \ge 1.5$ or $FC \le 0.67$. The p values were for reference. The bars show mean \pm SD. A two-sided t test was used.



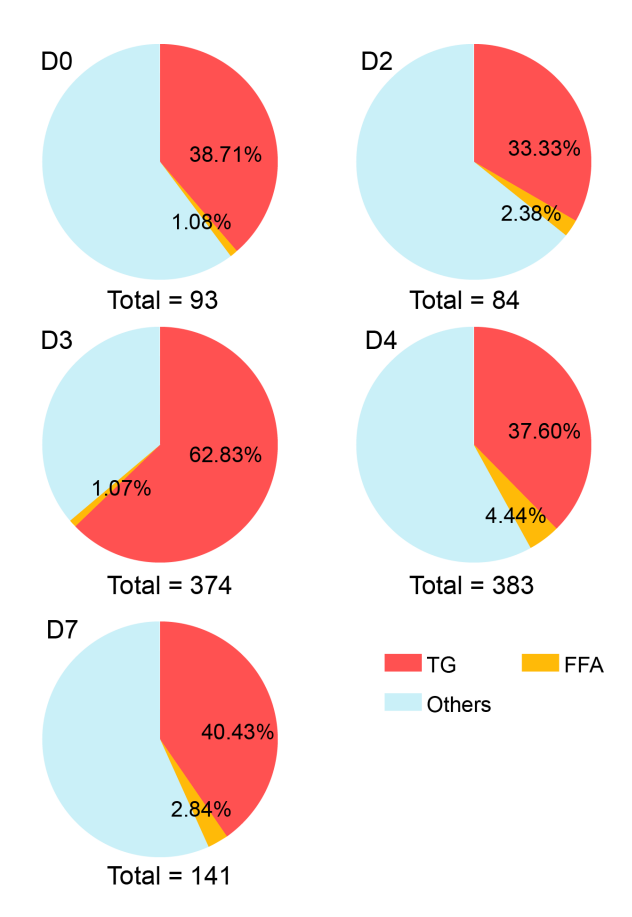
Supplementary Fig. 10 Changes of FFA contents in $EPASI^{+/+}$ mice at different time points in comparison with D0. A significant difference was determined based on VIP ≥ 1 , and FC ≥ 1.5 or FC ≤ 0.67 . The p values were for reference. The bars show mean \pm SD. A two-sided t test was used.



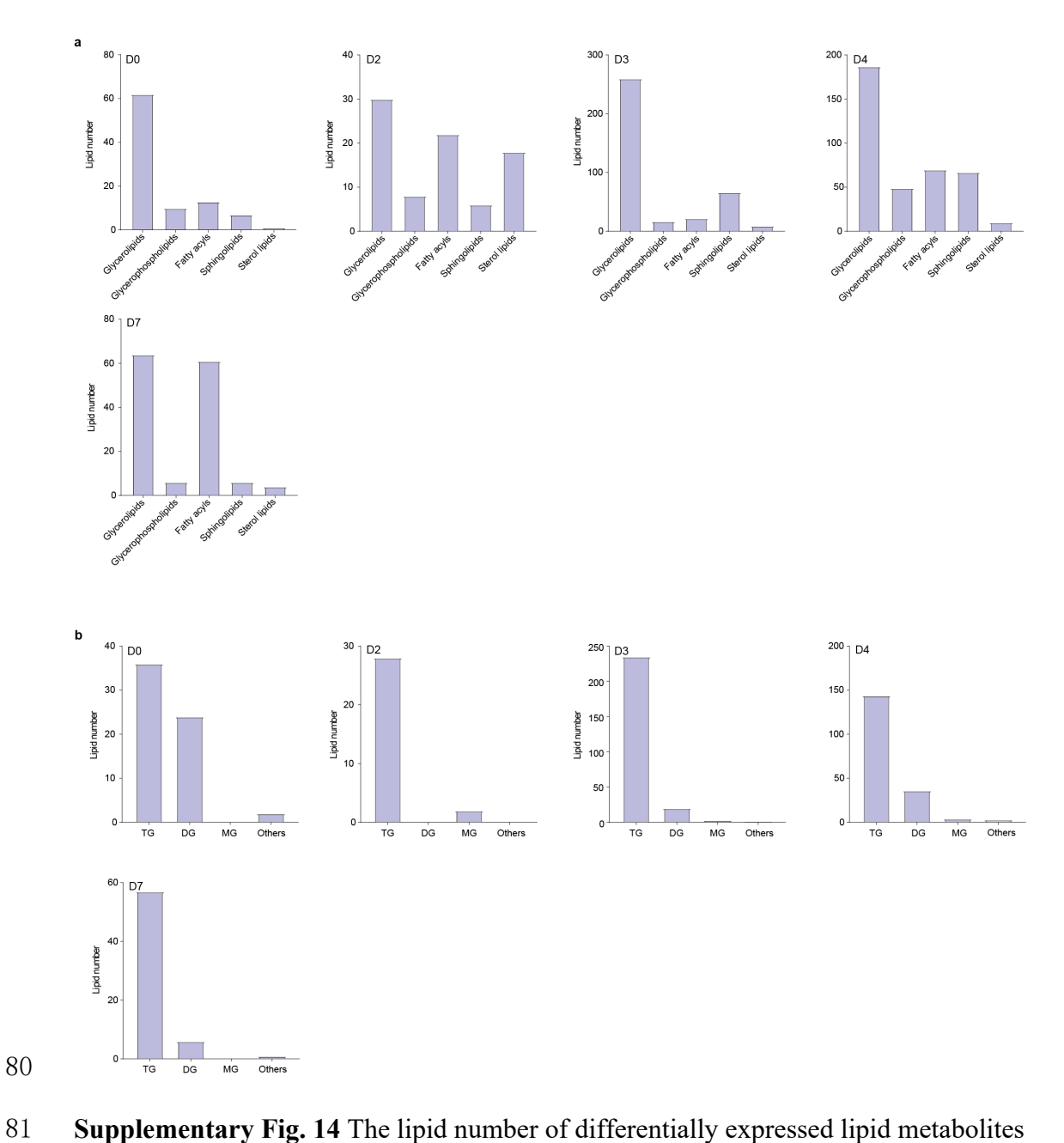
Supplementary Fig. 11 Content changes of FFA expressed both in mutant and wild type mice at different time points. A significant difference was determined based on VIP \geq 1, and FC \geq 1.5 or FC \leq 0.67. The p values were for reference. The bars show mean \pm SD. A two-sided t test was used.



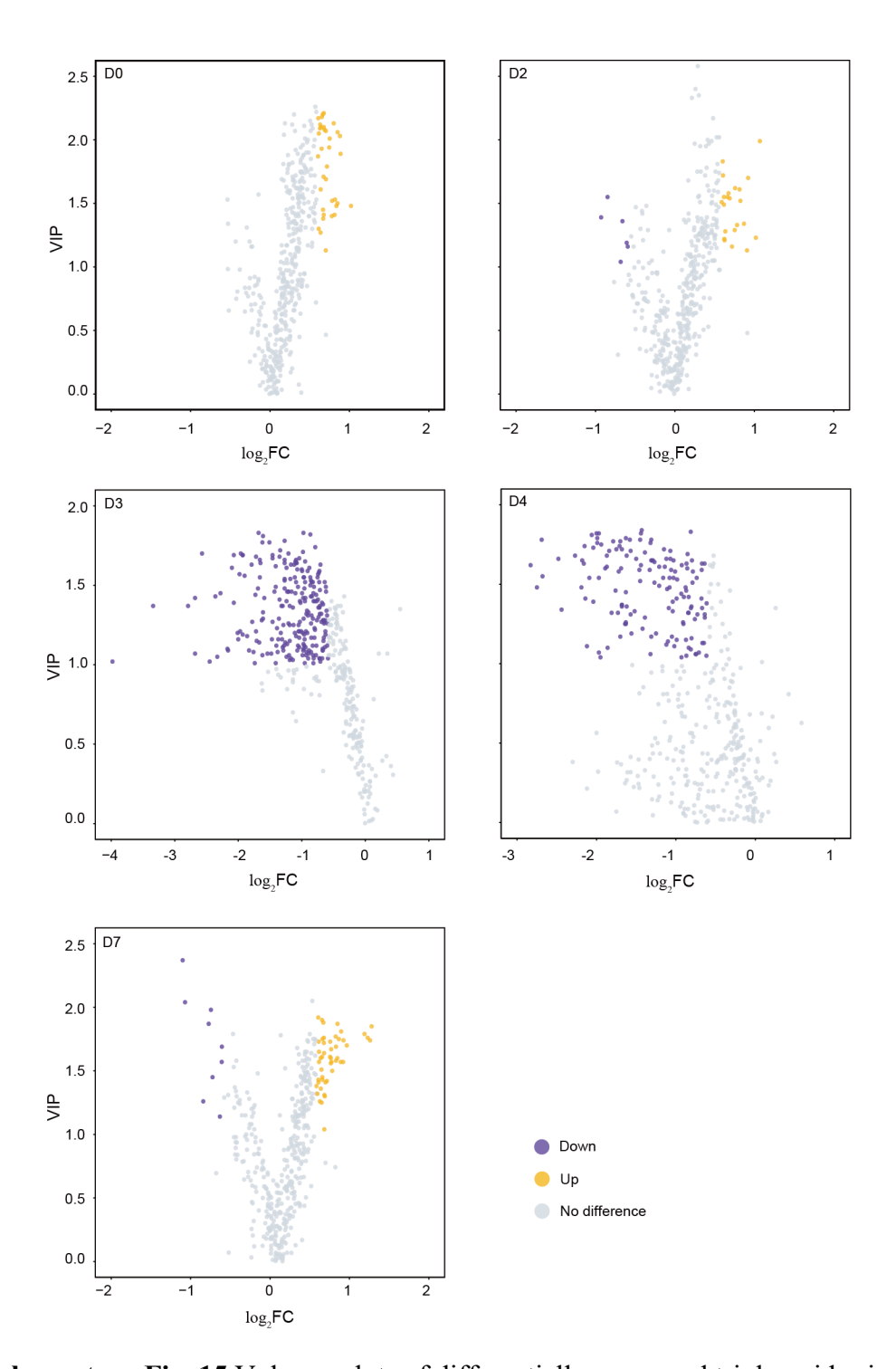
Supplementary Fig. 12 Changes of FFA contents in mutant and wild type mice on D3 (**a** and **b**) and D4 (**c** and **d**) detected using targeted lipidomics (n = 5 for each group). The bars show mean \pm SD. Two-sided Welch's t test was applied for **a**, two-sided t test for **b**, and two-sided Mann-Whitney U tests for **c** and **d**. Source data are provided as a **Source Data** file.



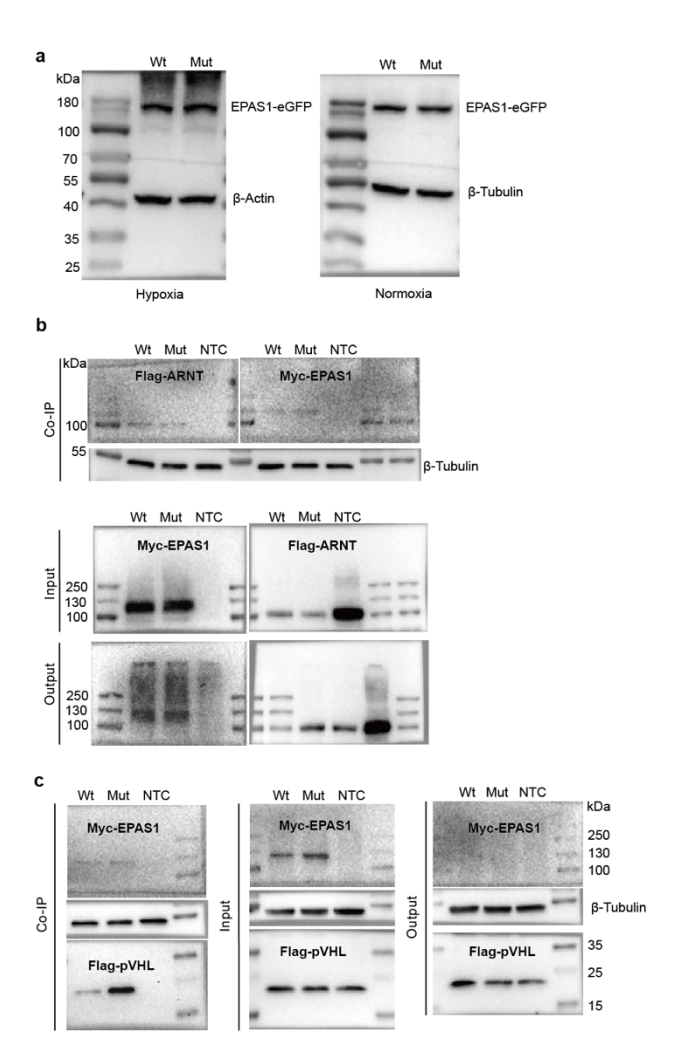
Supplementary Fig. 13 Percent of differentially expressed metabolites numbers of lipid between *EPASI*^{V162T/V162T} and *EPASI*^{+/+} mice at checked time points. "Total" refers to the total number of differentially expressed lipid metabolite subclasses detected between mutant and wild type mice.



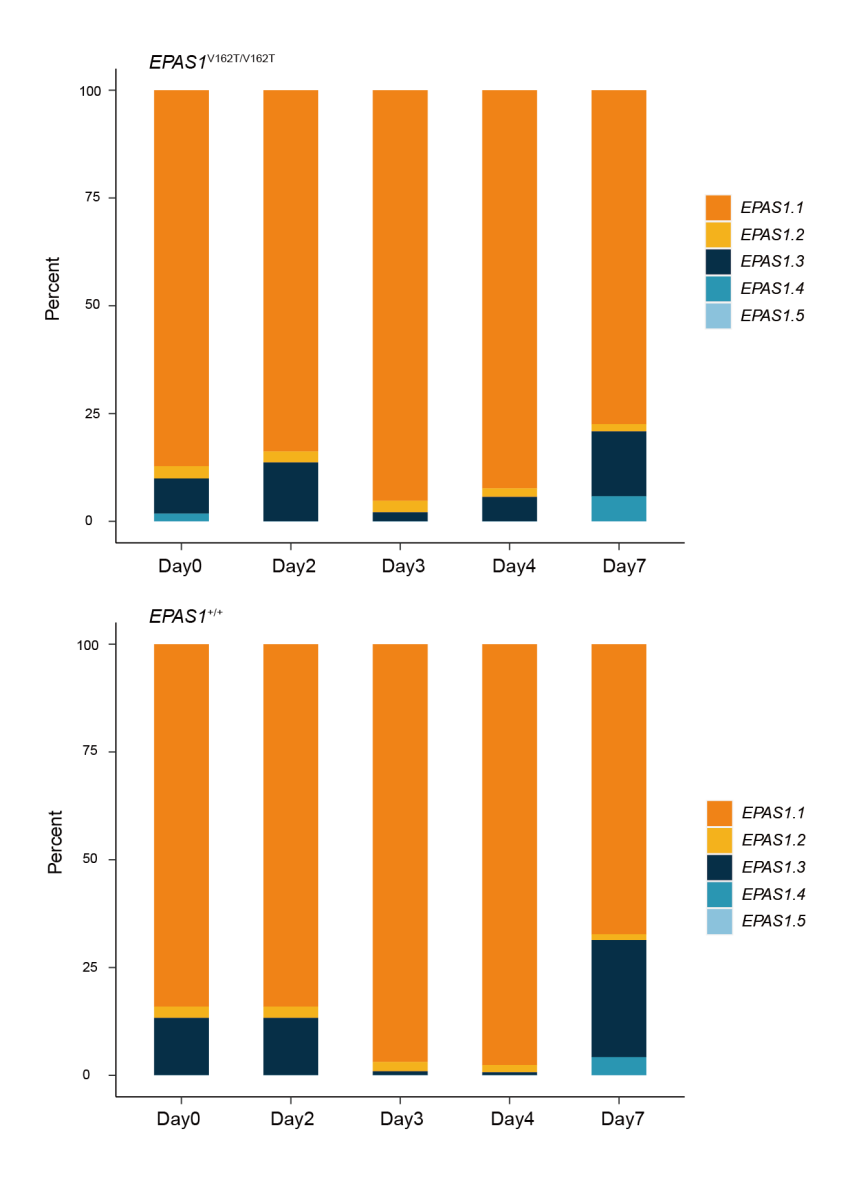
Supplementary Fig. 14 The lipid number of differentially expressed lipid metabolites (a) and glycerolipids (b) between *EPAS1*^{V162T/V162T} and *EPAS1*^{+/+} mice at each time point. TG: Triglyceride, DG: Diacylglycerol, MG: Monoacylglycerol.



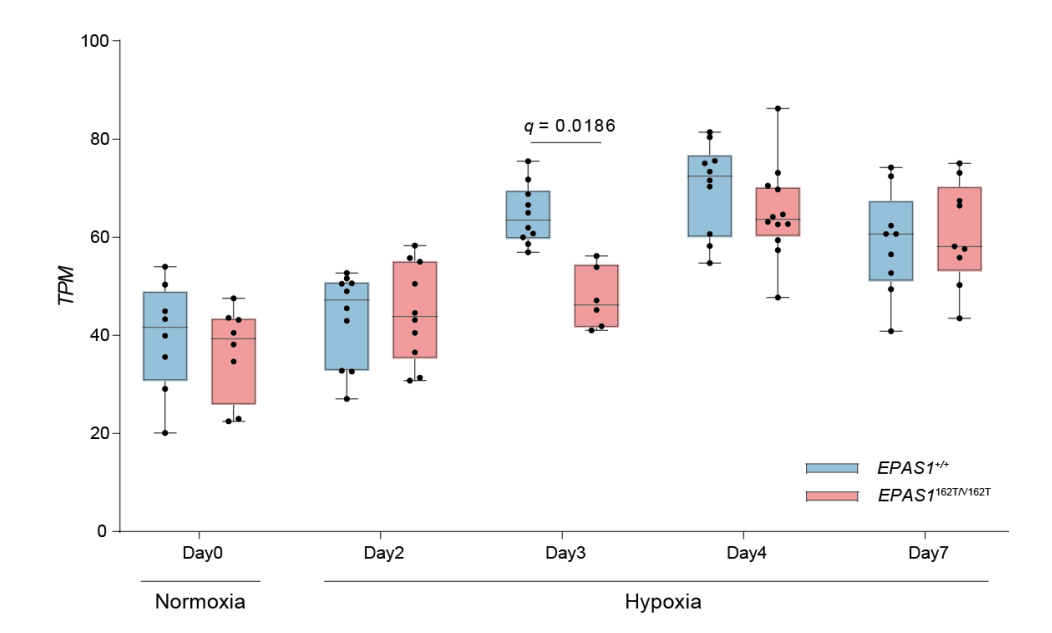
Supplementary Fig. 15 Volcano plots of differentially expressed triglycerides in liver samples between mutant and wild mice at each time point. The x-axis is the fold change (FC), and y-axis is the variable important in projection (VIP). A significant difference was determined based on VIP \geq 1, and FC \geq 1.5 or FC \leq 0.67.



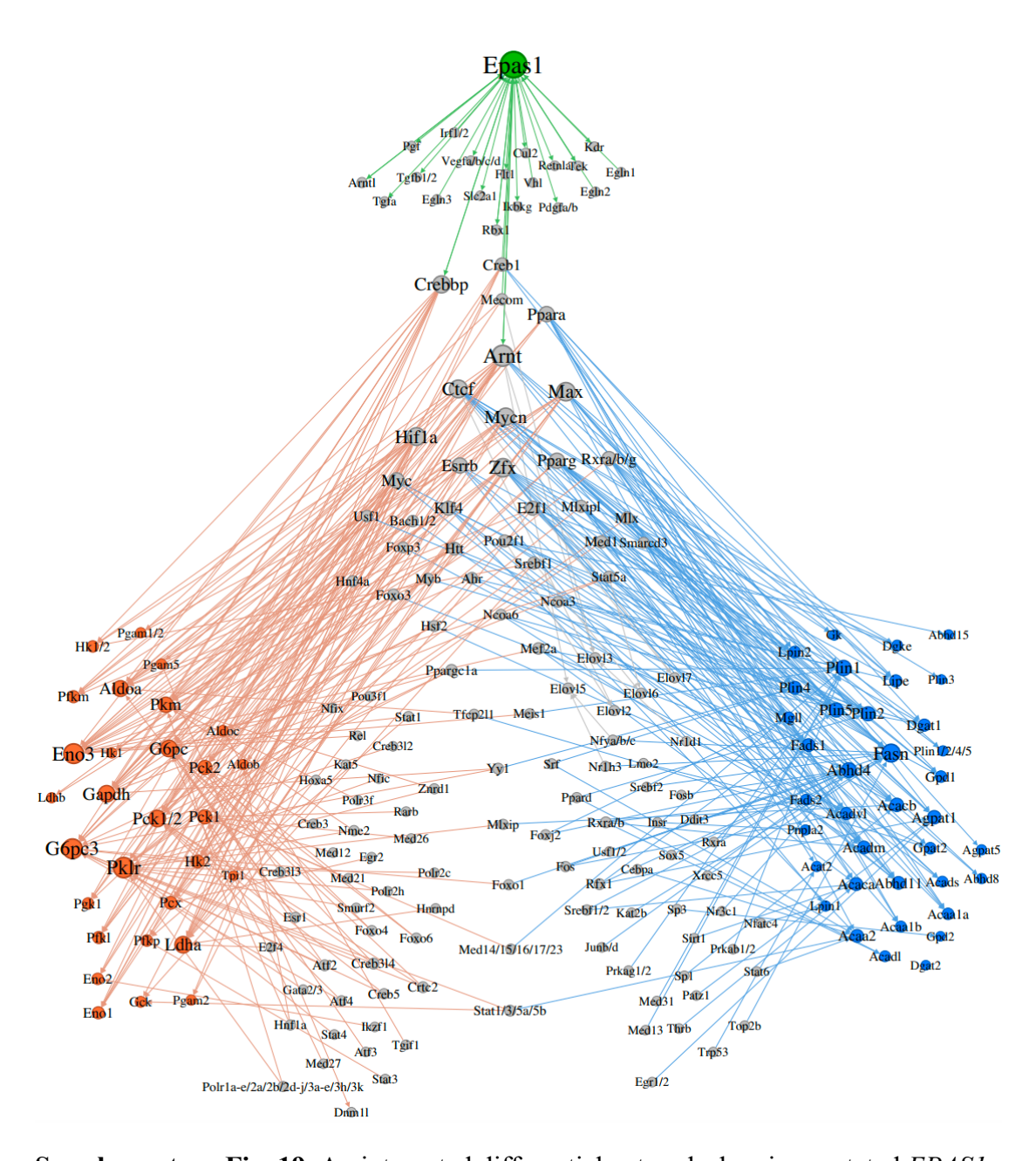
Supplementary Fig. 16 Expression of mutant and wild type EPAS1 proteins in Hela cells under normoxia and hypoxia conditions using GFP antibody, respectively (**a**). The EPAS1-eGFP fusion proteins internal control β-Actin and β-Tubulin protein are about 124 kDa, 43 kDa and 55 kDa, respectively. Co-immunoprecipitation (Co-IP) assay between EPAS1 and ARNT proteins (**b**). Co-IP assay between EPAS1 and VHL proteins (**c**). Myc-EPAS1 protein, Flag-ARNT protein and Flag-VHL protein are about 100 kDa, 88 kDa and 22 kDa, respectively. Wt: EPAS1^{+/+}, Mut: EPAS1^{V162T/V162T}, NTC: negative control.



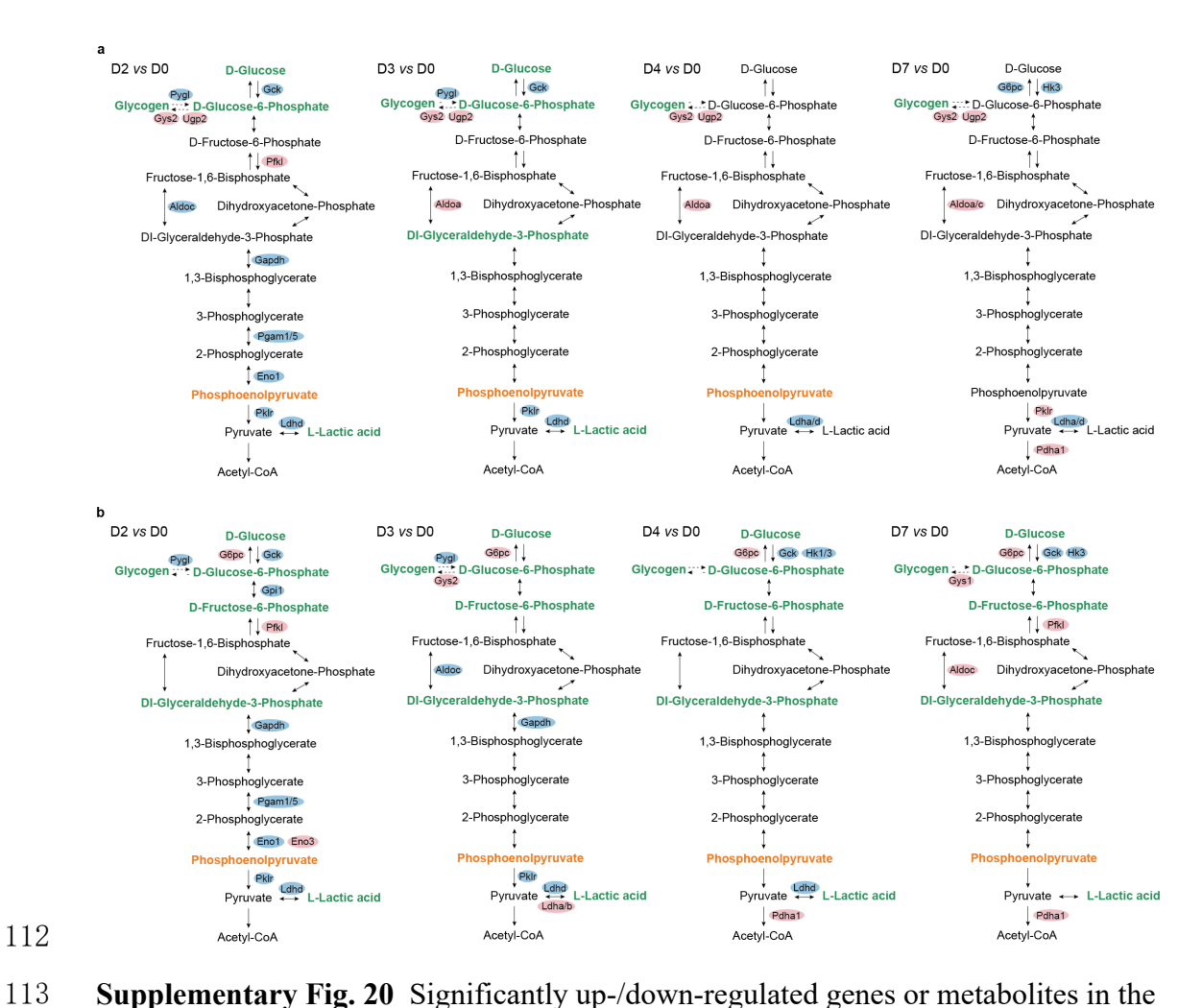
Supplementary Fig. 17 Percentages of each *EPAS1* transcript expression in mutant and wild type mice at each time point. Source data are provided as a **Source Data** file.



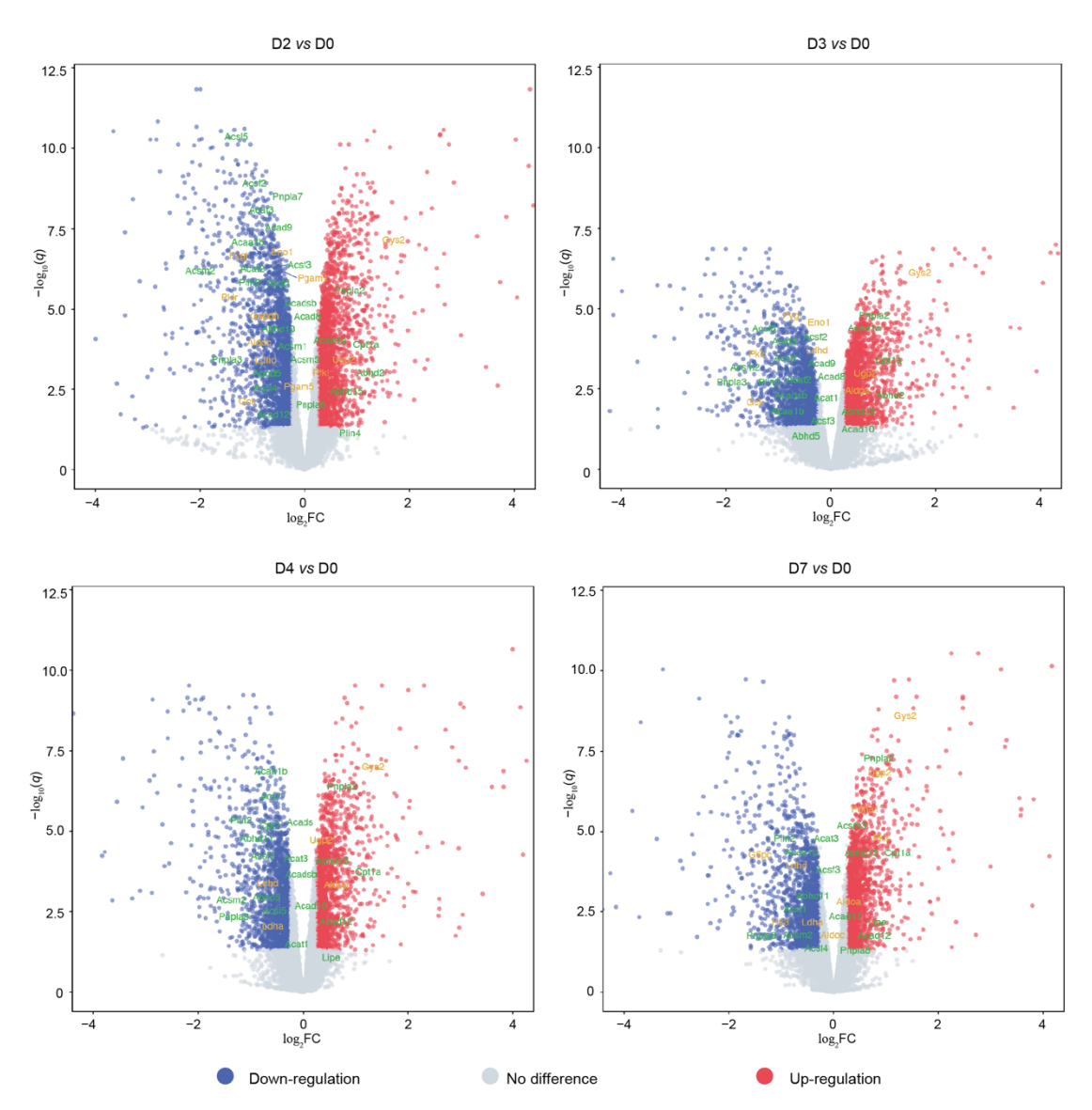
Supplementary Fig. 18 Expression differences of *EPAS1.1* transcript between mutant and wild type mice at each time point. *TPM*: the transcripts per million. A significant difference was determined by fold change ≥ 1.2 , and q < 0.05. Source data are provided as a **Source Data** file.



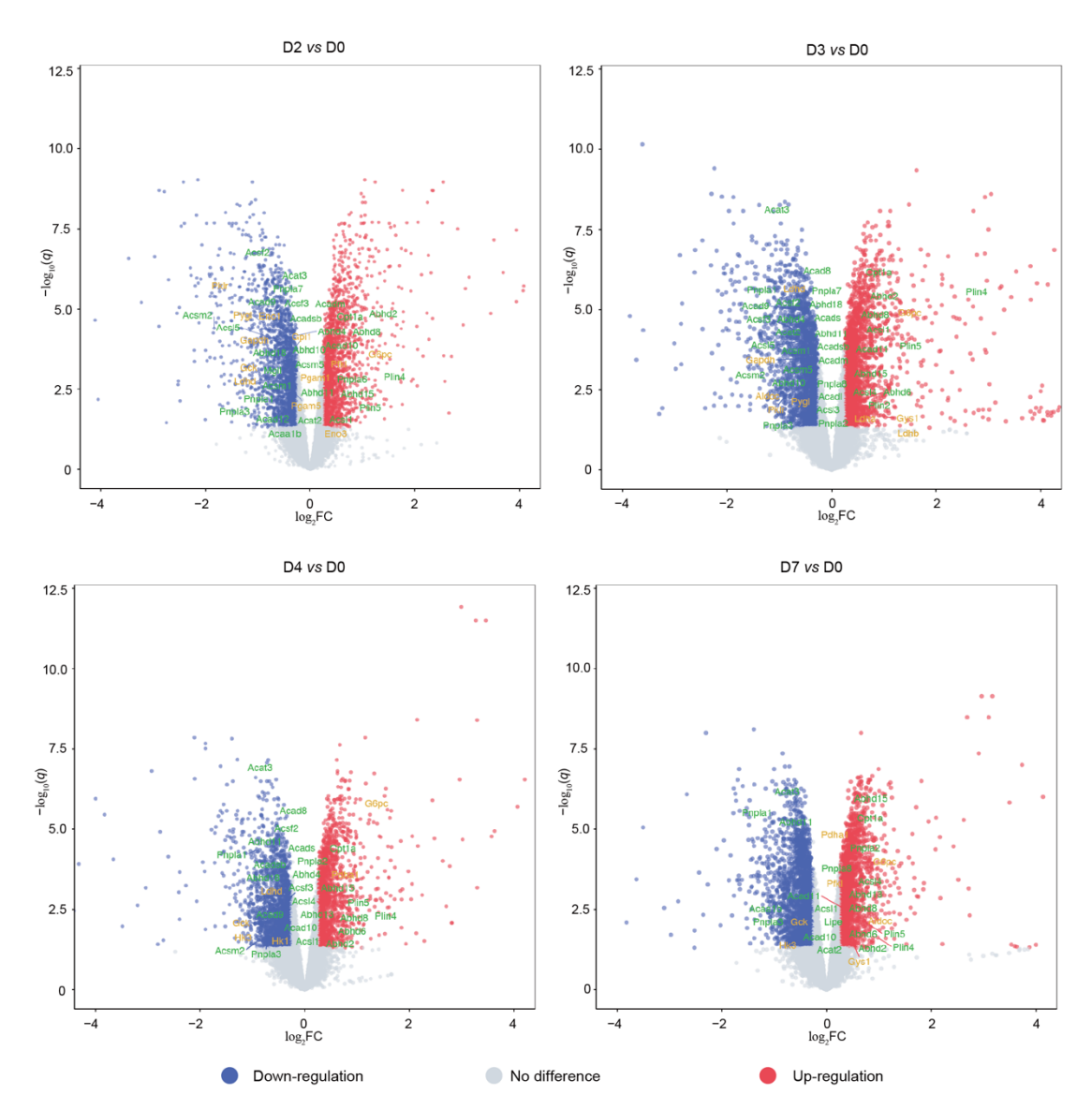
Supplementary Fig. 19 An integrated differential network showing mutated *EPAS1* affect gene regulation related to glucose and lipid metabolism using differential network analysis on mutant and wild mice from D0 to D7. *EPAS1* is shown in green, and orange and blue circles represent genes involved in glucose and lipid metabolism pathways, respectively. Source data are provided as a **Source Data** file.



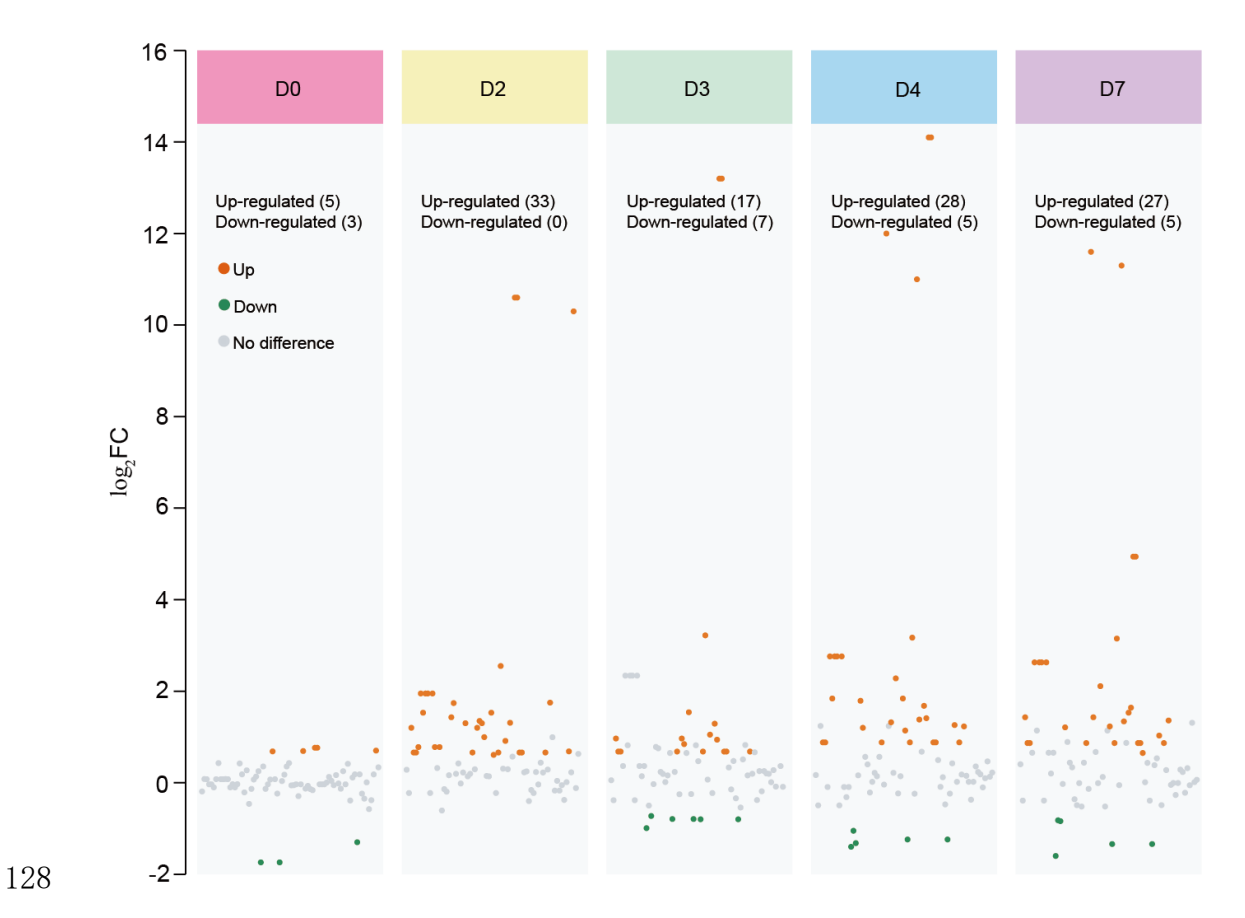
Supplementary Fig. 20 Significantly up-/down-regulated genes or metabolites in the glucose metabolic pathways in (a) mutant and (b) wild type mice livers from D2 to D7 in comparison with D0, respectively. Up- and down-regulated genes in both types of mice are in pink and blue, respectively, and up- and down-regulated carbohydrate metabolites are in orange and green, respectively.



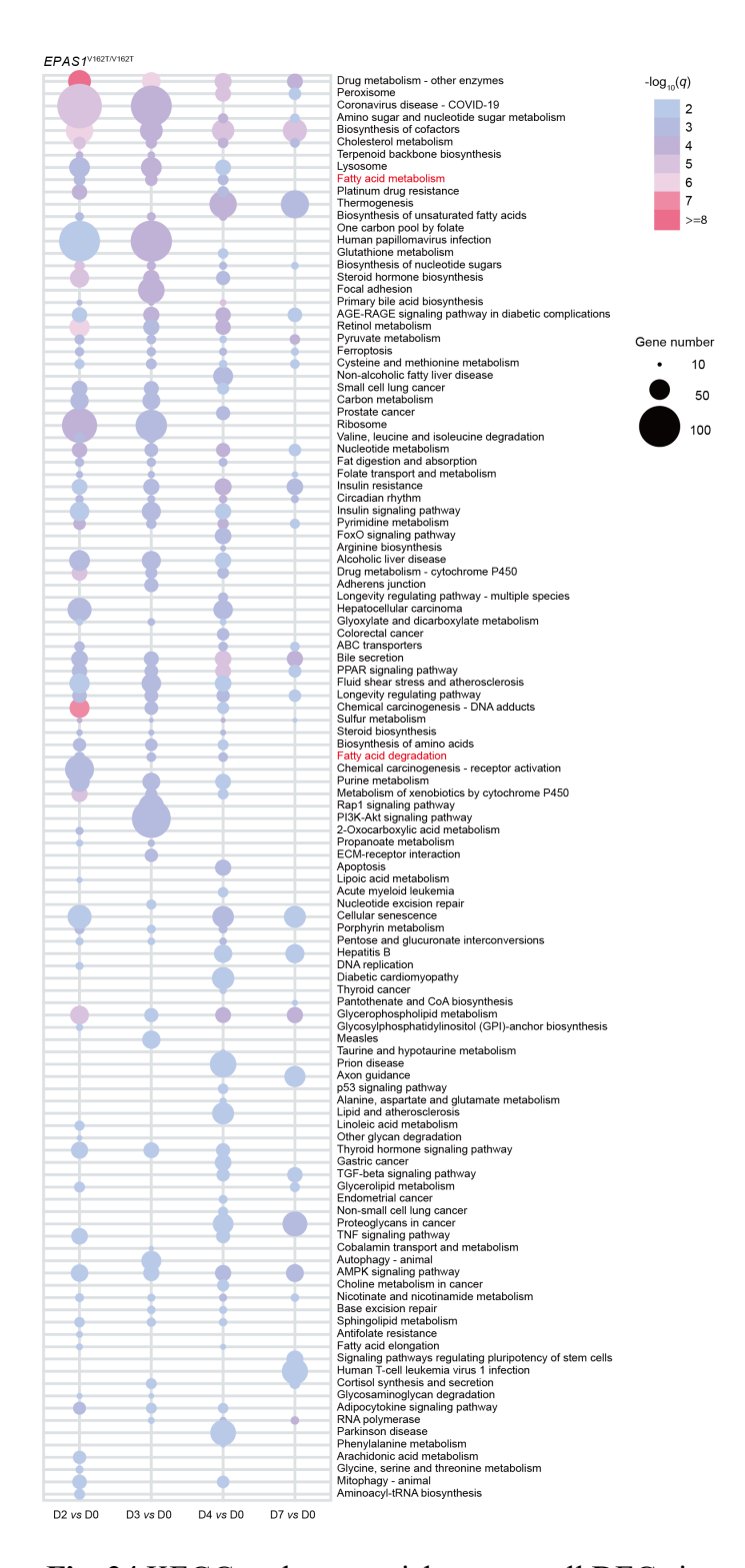
Supplementary Fig. 21 Volcano plots for differential expression level of each gene in hepatic samples of mutant mice ($EPASI^{V162T/V162T}$) from D2 to D7 in comparison with D0, respectively. The x-axis is the fold change (log_2FC), $|log_2FC| \ge 0.26$ and y-axis is the q value, the probability that a gene has a statistical significance.



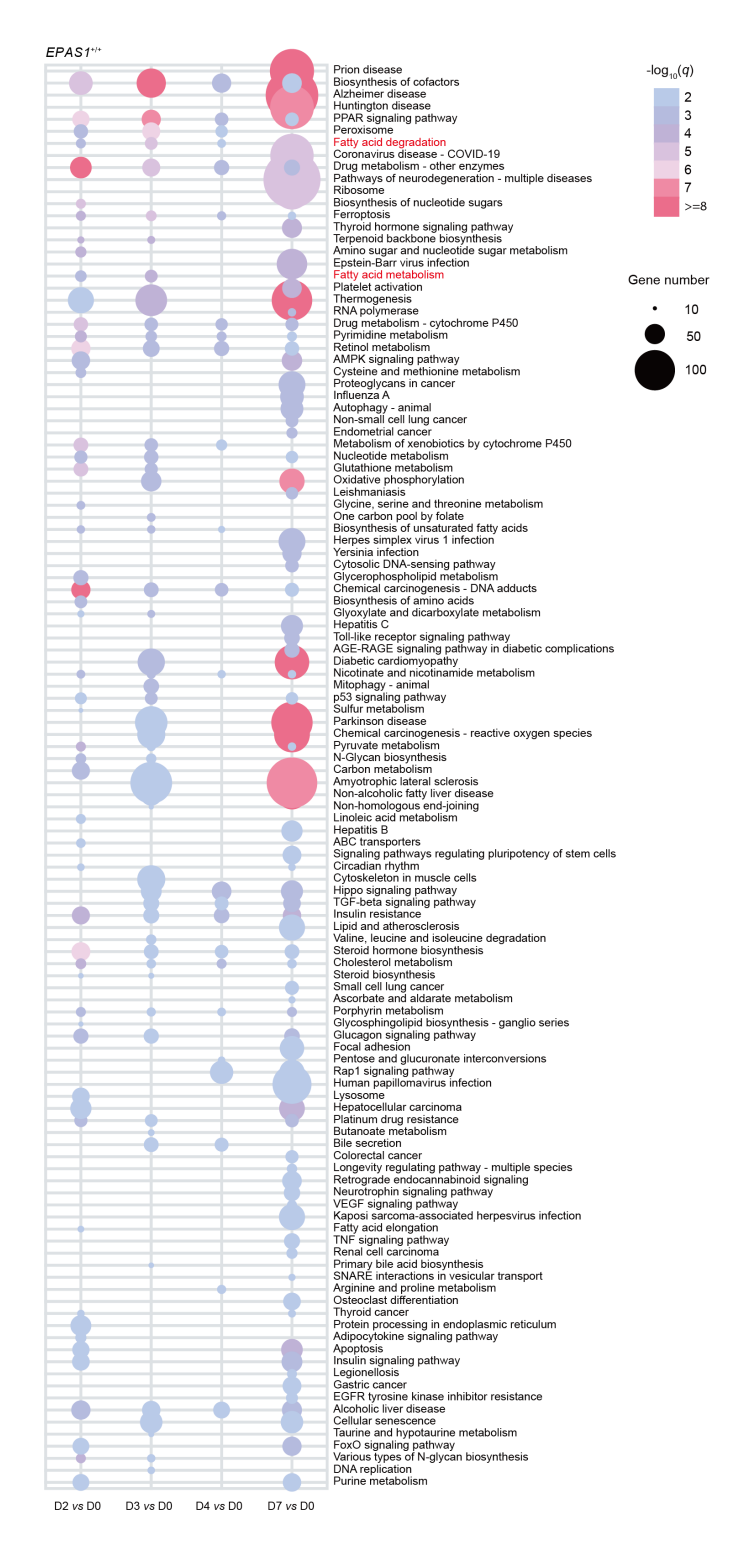
Supplementary Fig. 22 Volcano plots for differential expression level of each gene in hepatic samples of wild type mice ($EPASI^{+/+}$) from D2 to D7 in comparison with D0, respectively. The x-axis is the fold change (log_2FC), $|log_2FC| \ge 0.26$ and y-axis is the q value, the probability that a gene has a statistical significance.



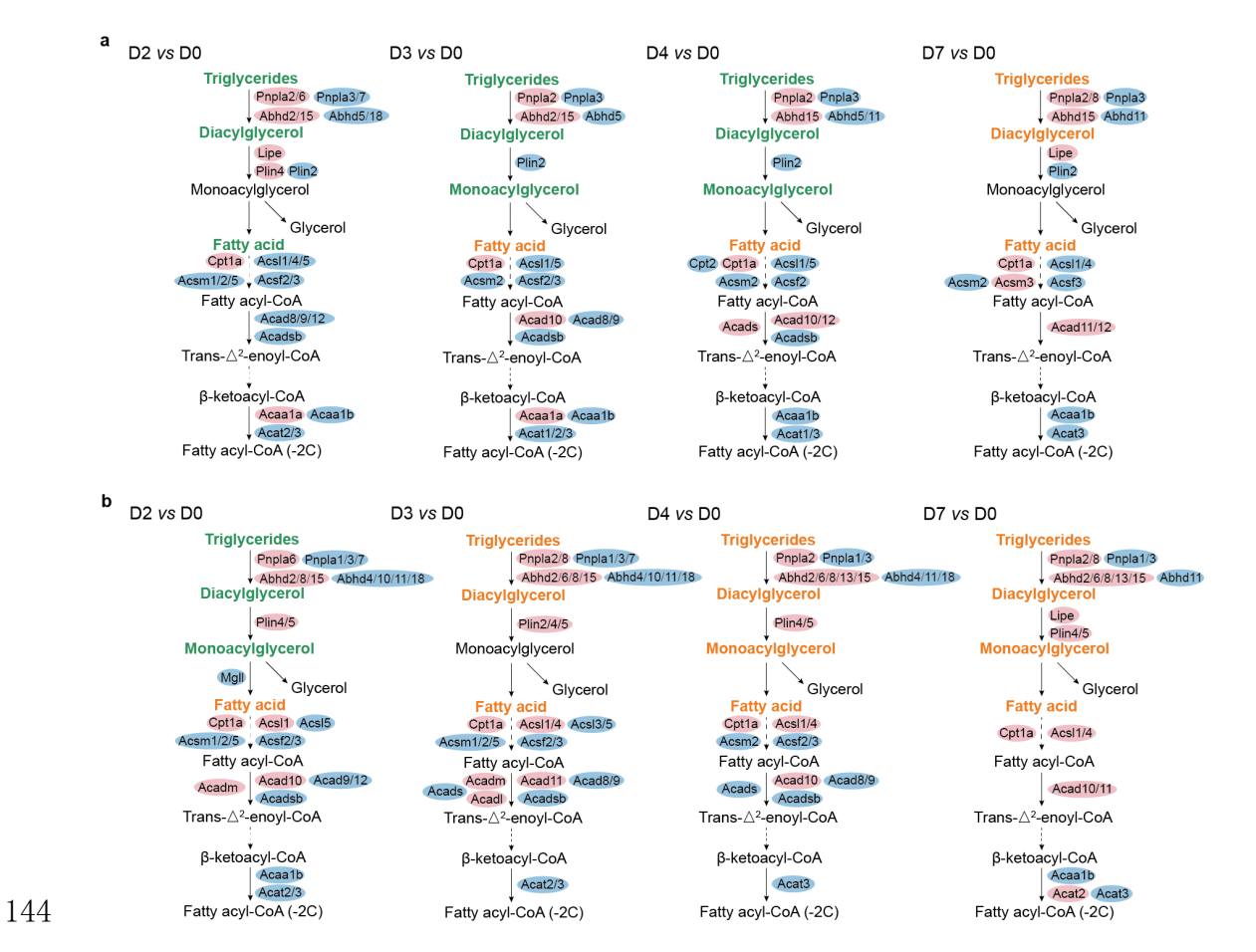
Supplementary Fig. 23 Volcano plots of differentially expressed carbohydrate metabolites in mutant and wild type mice under normoxia (D2-D7) and hypoxia (D0). The y-axis is fold change (log₂FC). A significant difference in expression level between mouse types was determined by variable important in projection value ≥ 1 , and FC being ≥ 1.5 or FC ≤ 0.67 .



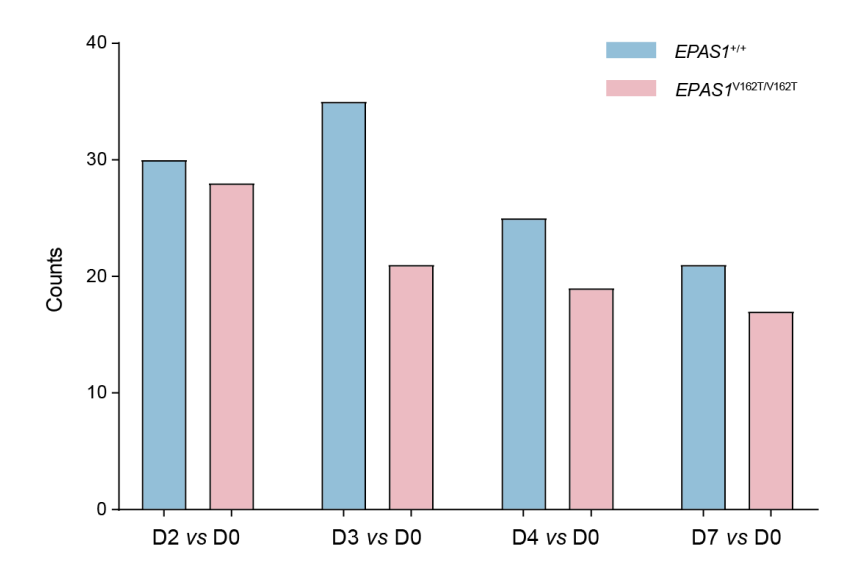
Supplementary Fig. 24 KEGG pathway enrichment on all DEGs in mutant mice liver in comparison with D0 at each time point. Circle size represents the gene number enriched in each pathway. A hypergeometric test and FDR adjustment were applied. Source data are provided as a **Source Data** file.



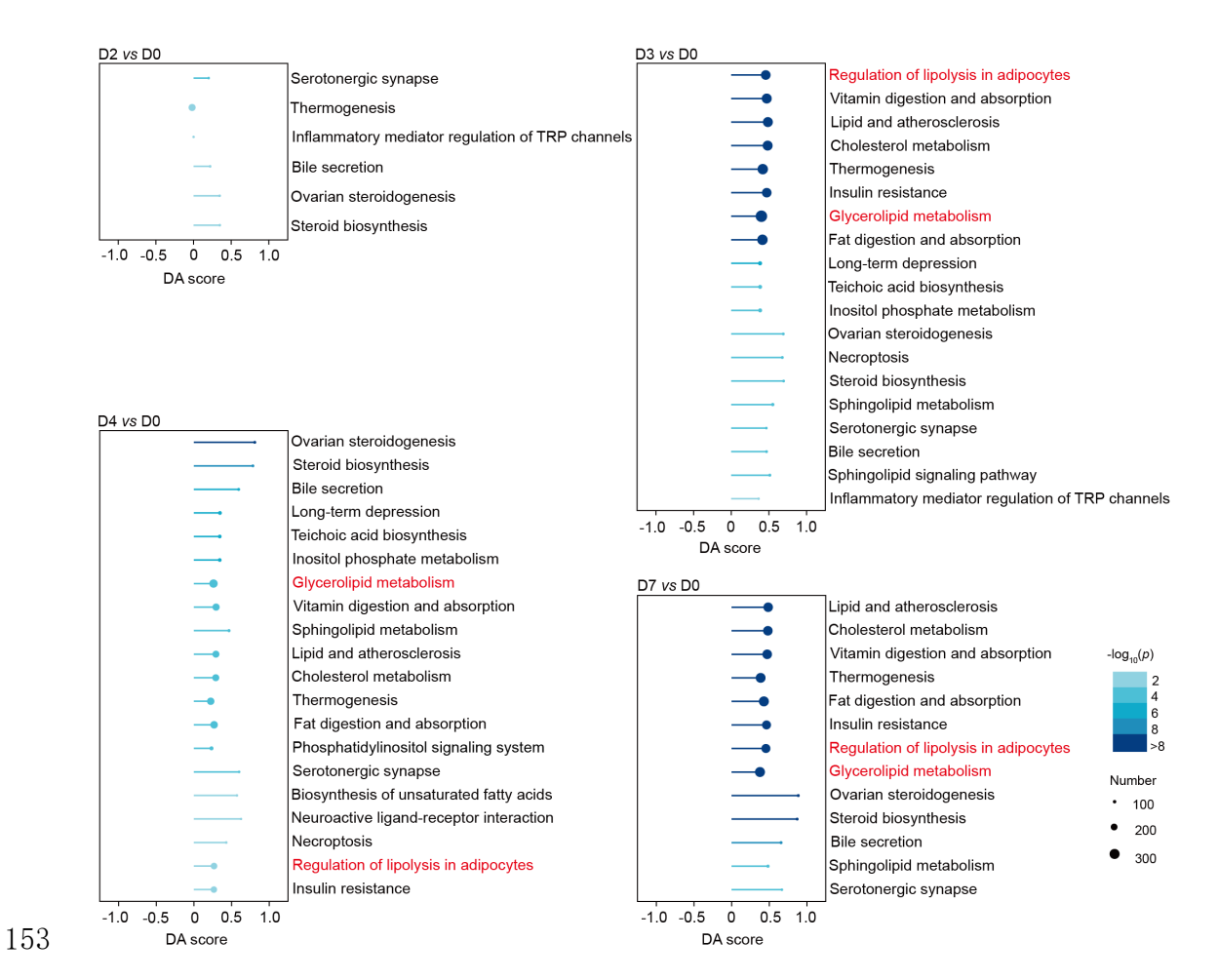
Supplementary Fig. 25 KEGG pathway enrichment on all DEGs in wild type mice liver in comparison with D0 at each time point. Circle size represents the gene number enriched in each pathway. A hypergeometric test and FDR adjustment were applied. Source data are provided as a **Source Data** file.



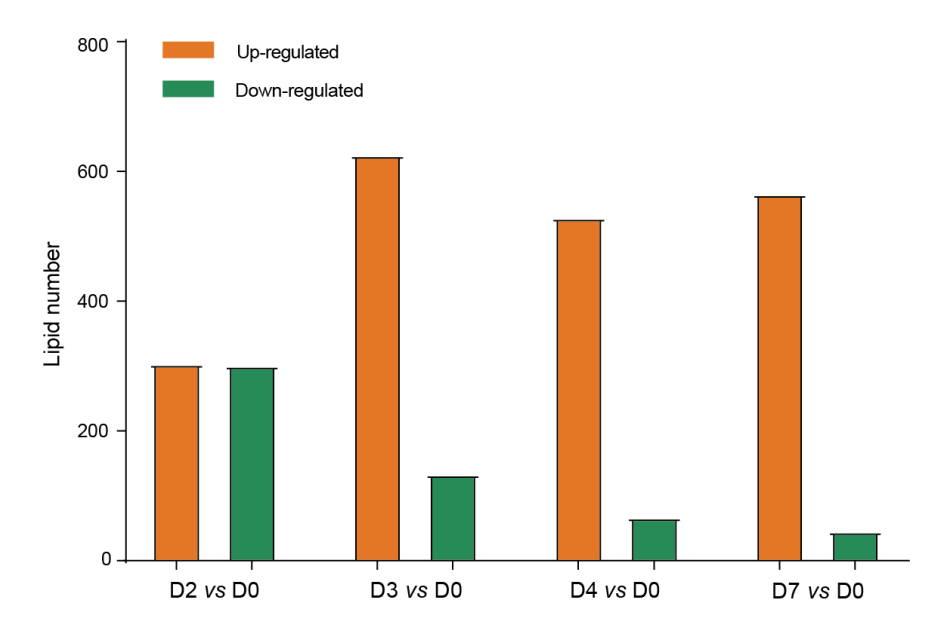
Supplementary Fig. 26 Significantly up-/down-regulated genes or metabolites in the FFA metabolic pathways in mutant and (a) wild type mice livers (b) from D2 to D7 in comparison with D0, respectively. Up- and down-regulated genes in both types of mice are in pink and blue, respectively, and up- and down-regulated lipid metabolites are in orange and green, respectively.



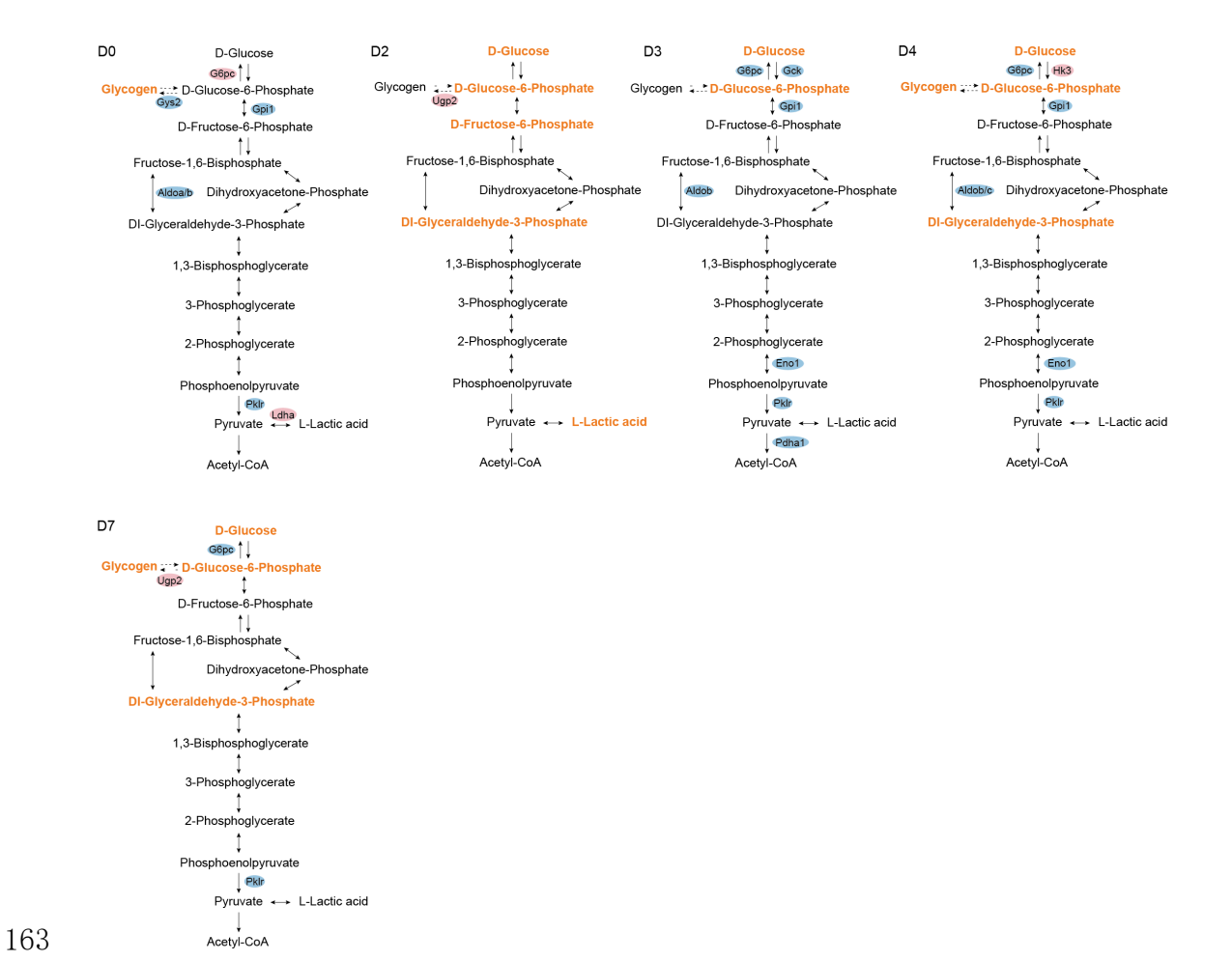
Supplementary Fig. 27 Count comparison of DEGs that were related to FFA metabolic pathways in comparison with D0 between mutant and wild type mice.



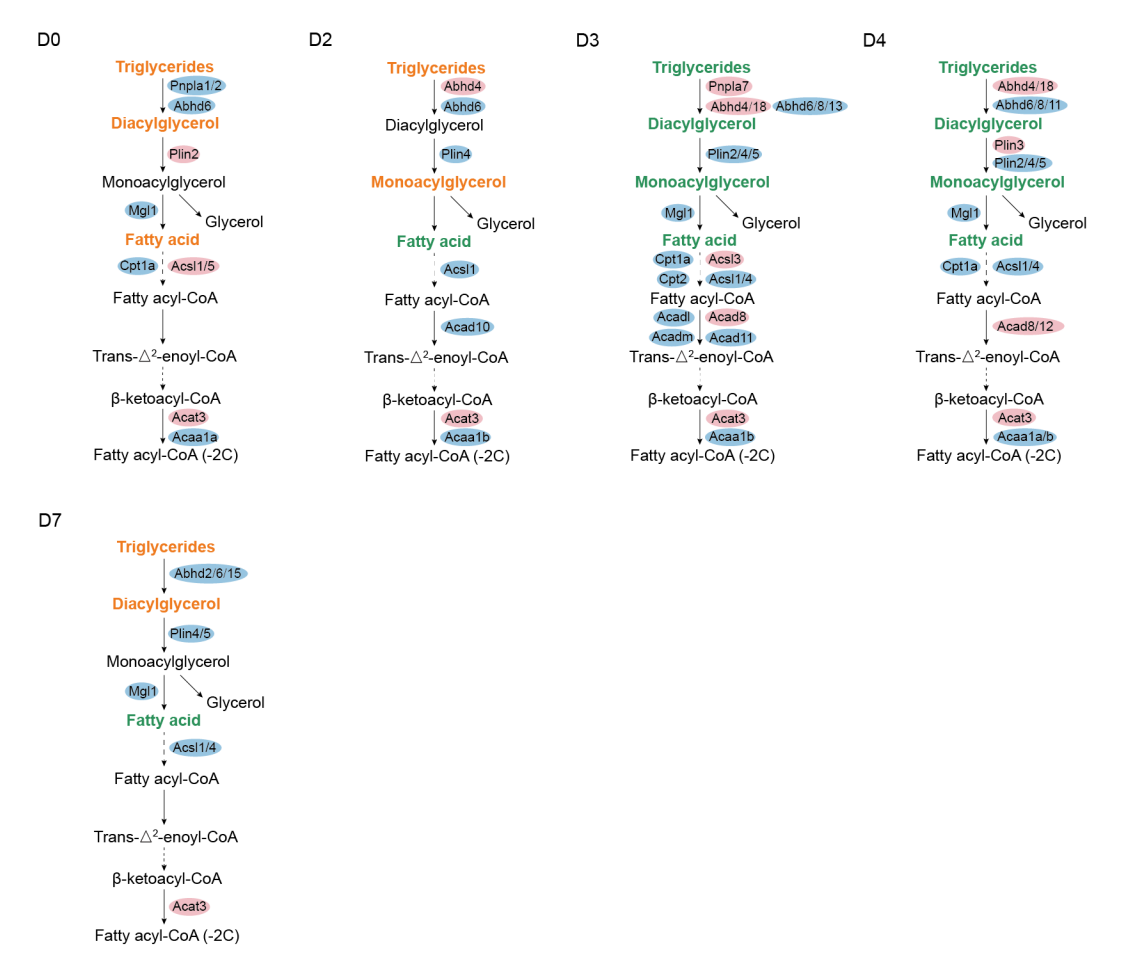
Supplementary Fig. 28 KEGG enrichment analysis on all differentially expressed lipid metabolites in wild type mice at each time point in comparison with D0. X-axis shows the enrichment score. Circles represent the number of metabolites enriched. Source data are provided as a Source Data file.



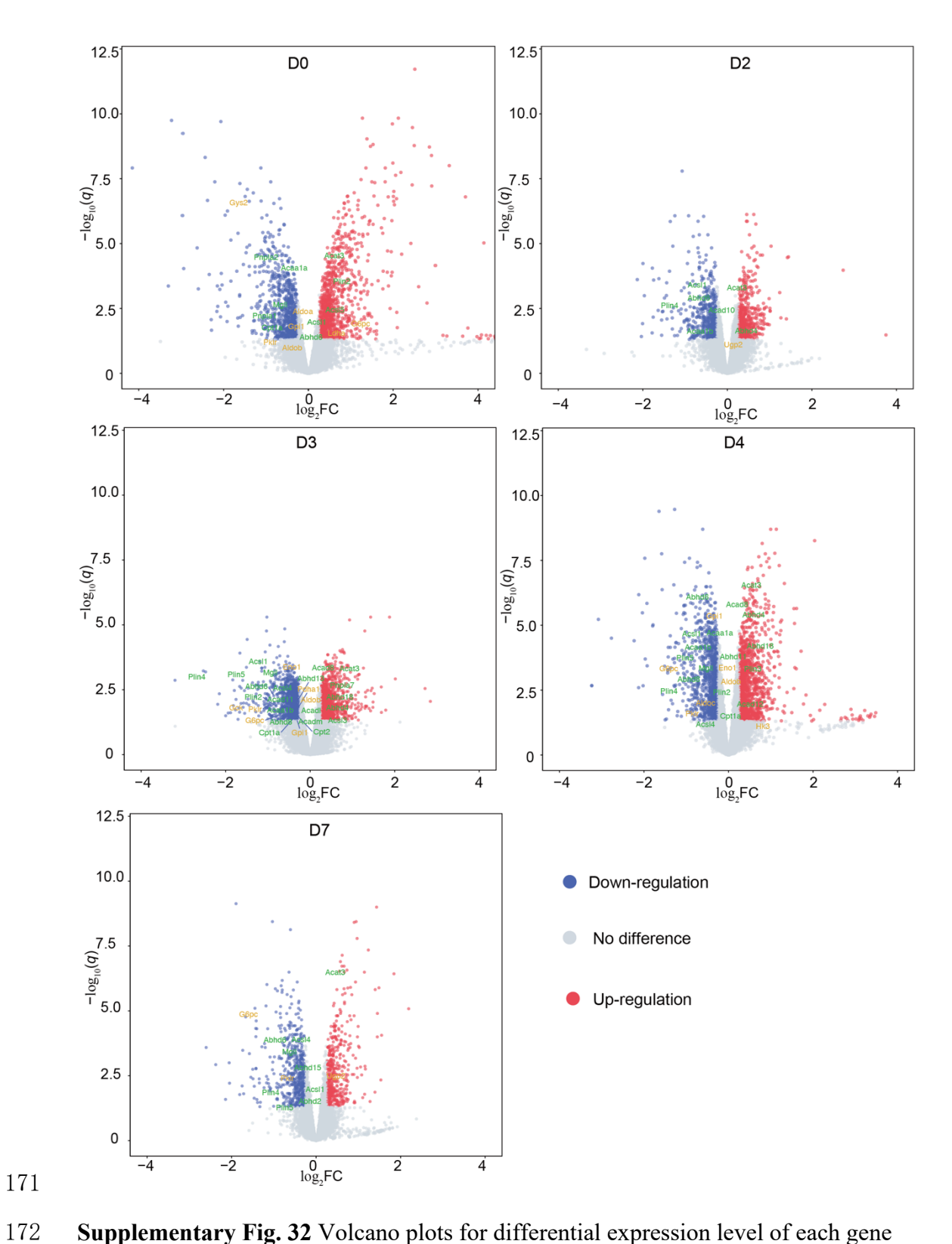
Supplementary Fig. 29 The number of differentially expressed lipid metabolites in wild type mice at each time point in comparison with D0. The total number means the number of differentially expressed lipid metabolites detected between hypoxic treatments and normoxic controls.



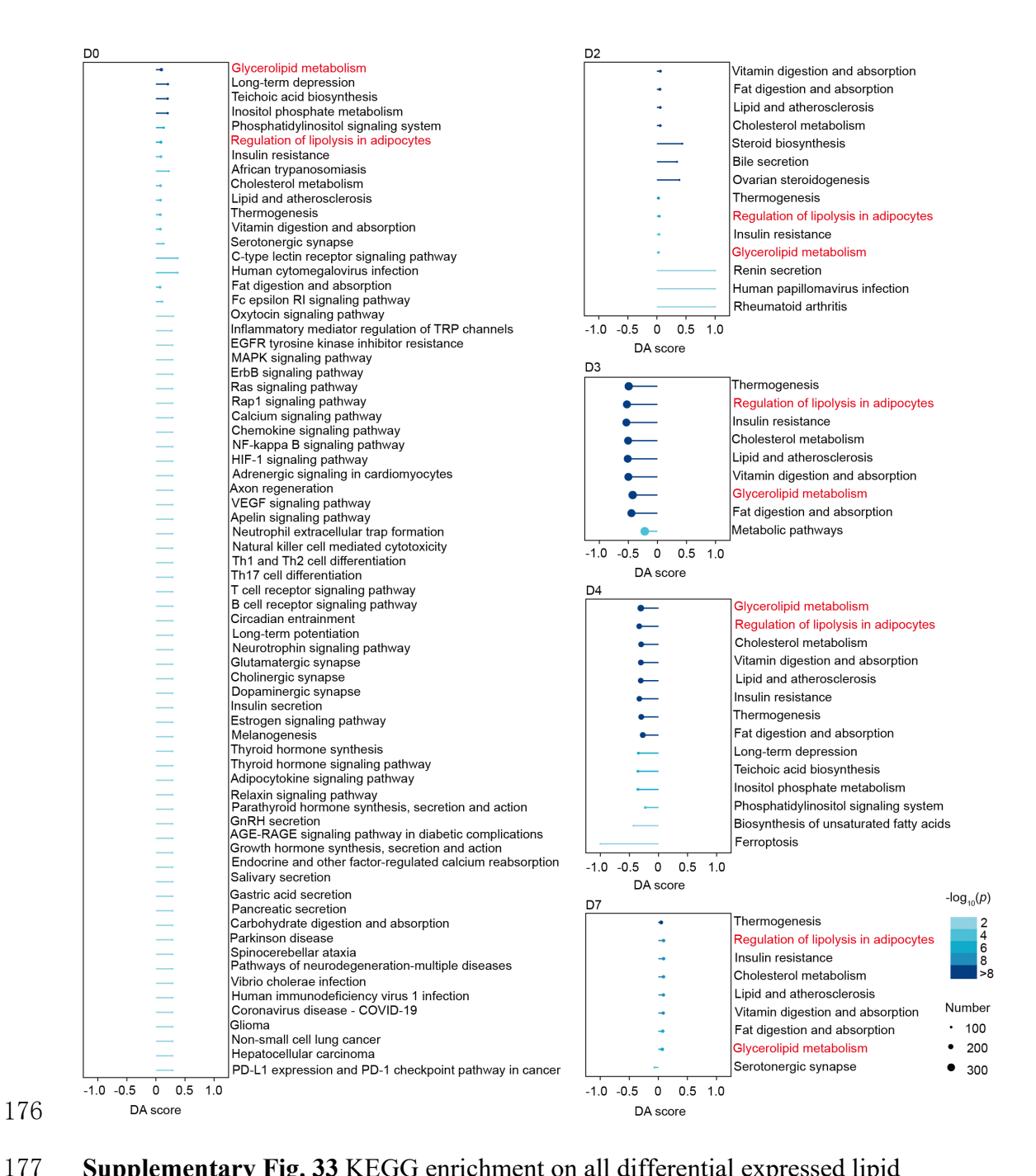
Supplementary Fig. 30 Significantly up-/down-regulated genes (pink and blue) or metabolites (orange and green) in the glucose metabolic pathways between mutant and wild type mice livers from D0 to D7.



Supplementary Fig. 31 Significantly up-/down-regulated genes (pink and blue) or metabolites (orange and green) in the lipid metabolic pathways between mutant and wild type mice livers from D0 to D7.

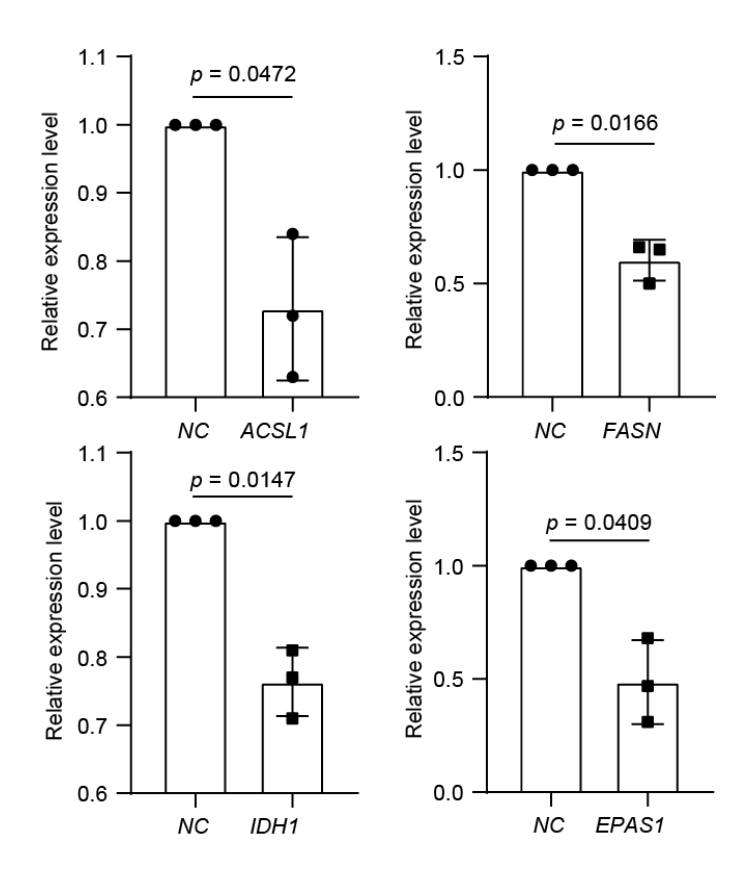


Supplementary Fig. 32 Volcano plots for differential expression level of each gene in hepatic samples between mutant ($EPASI^{V162T/V162T}$) and wild type ($EPASI^{+/+}$) mice from D0 to D7. The x-axis is the fold change (log_2FC), $|log_2FC| \ge 0.26$ and y-axis is the q value, the probability that a gene has a statistical significance.

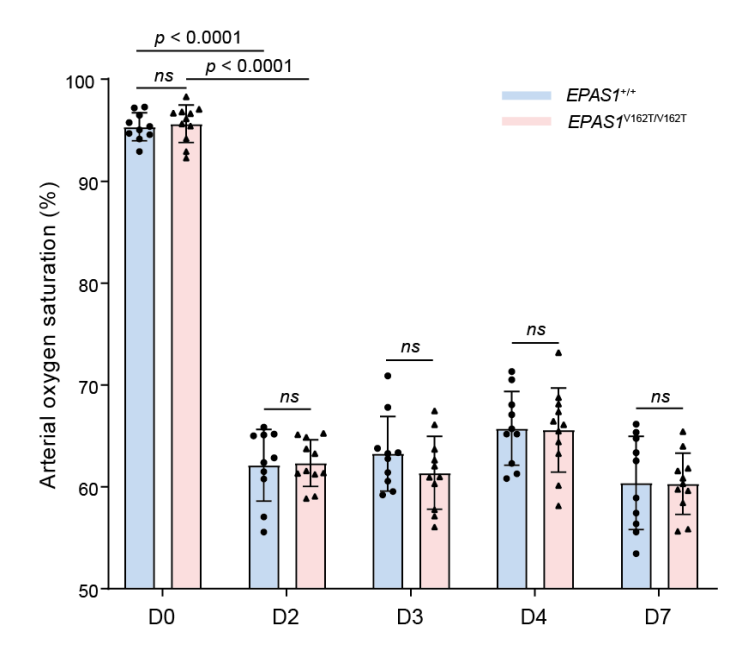


Supplementary Fig. 33 KEGG enrichment on all differential expressed lipid metabolites in *EPAS1*^{V162T/V162T} mice compared to *EPAS1*^{+/+} mice at each time point.

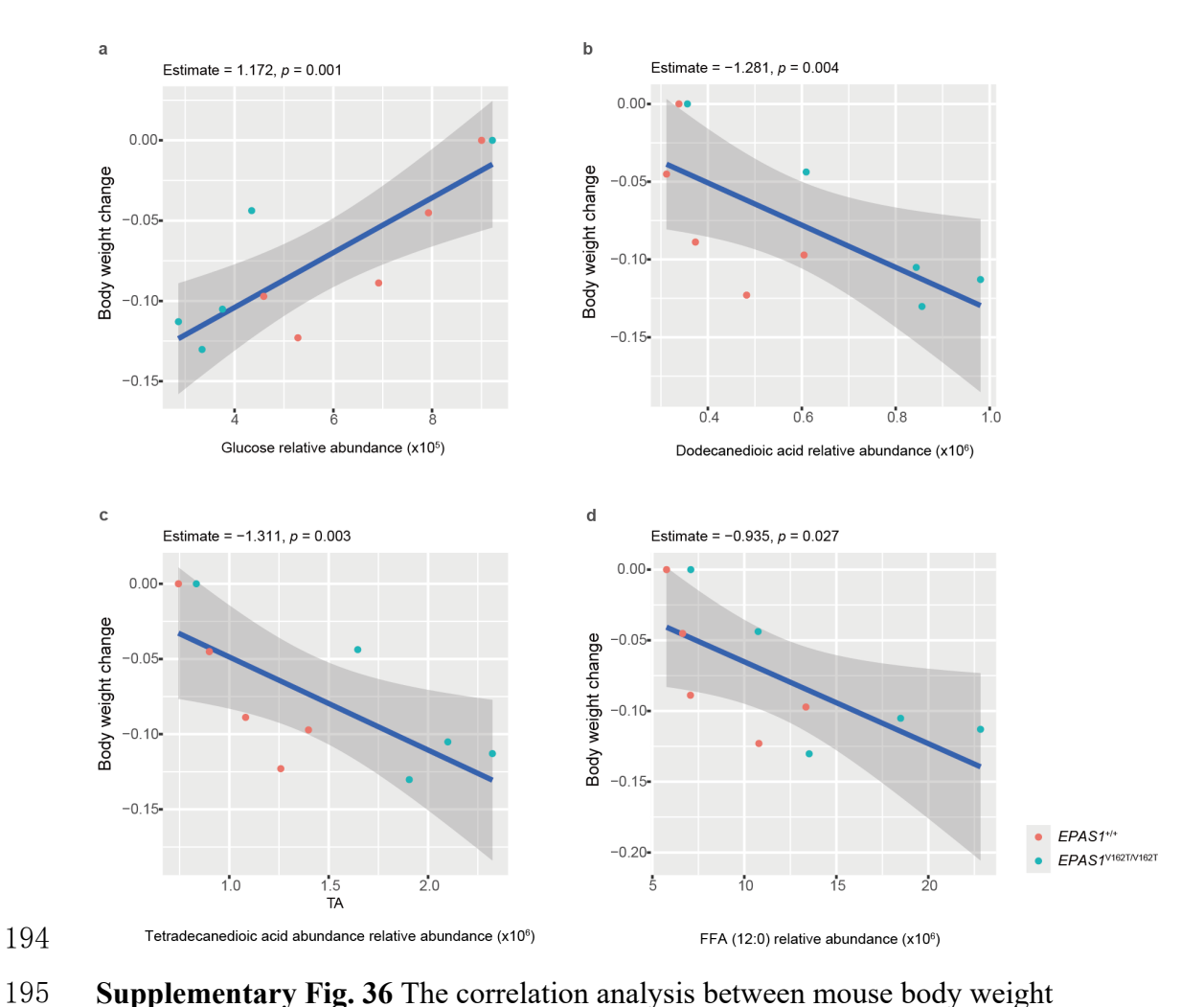
X-axis shows the enrichment score. Circles represent the number of metabolites enriched. Source data are provided as a **Source Data** file.



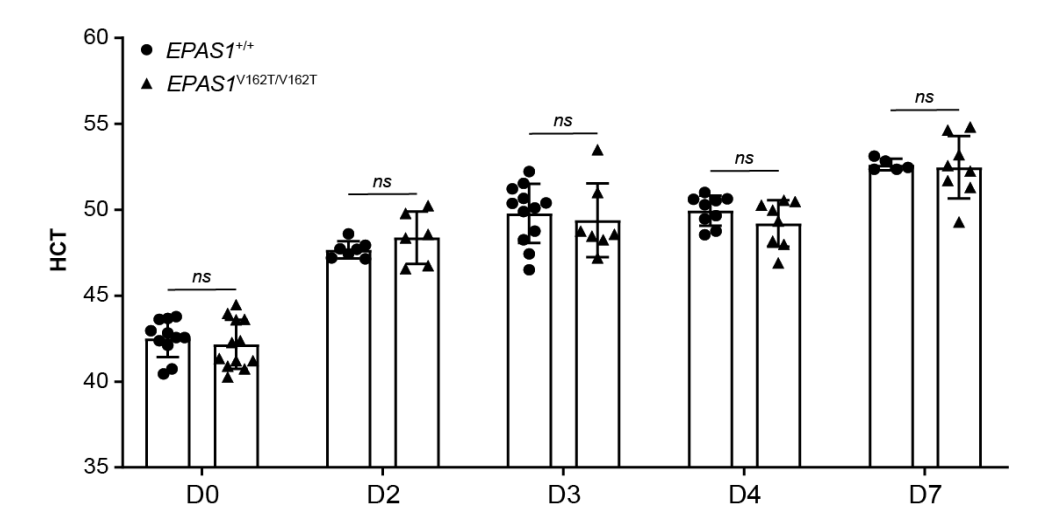
Supplementary Fig. 34 qPCR results of relative expression level of genes involved in lipid metabolism. ACSL1: acyl-CoA synthetase long chain family member 1, FASN: fatty acid synthase, IDH1: isocitrate dehydrogenase (NADP (+)) 1. The bars show mean \pm SD and two-sided t tests were applied. Source data are provided as a **Source Data** file.



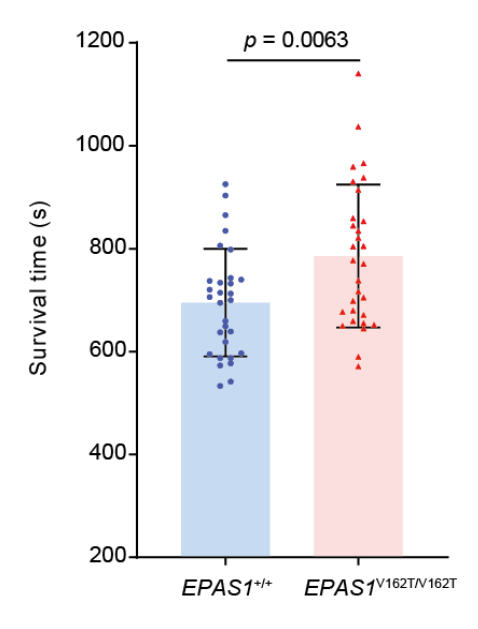
Supplementary Fig. 35 Comparisons of arterial oxygen saturation between $EPASI^{V162T/V162T}$ (n = 11) and $EPASI^{+/+}$ (n = 10) mouse individuals under normoxia and hypoxia. The bars display mean \pm SD. Two-sided Welch's t test was applied for the testing D2 vs D0 in wild type mice and two-sided t tests for the remaining. ns: no significant difference. P values for each group were 0.6723, 0.8691, 0.2483, 0.9249 and 0.9606. Source data are provided as a **Source Data** file.



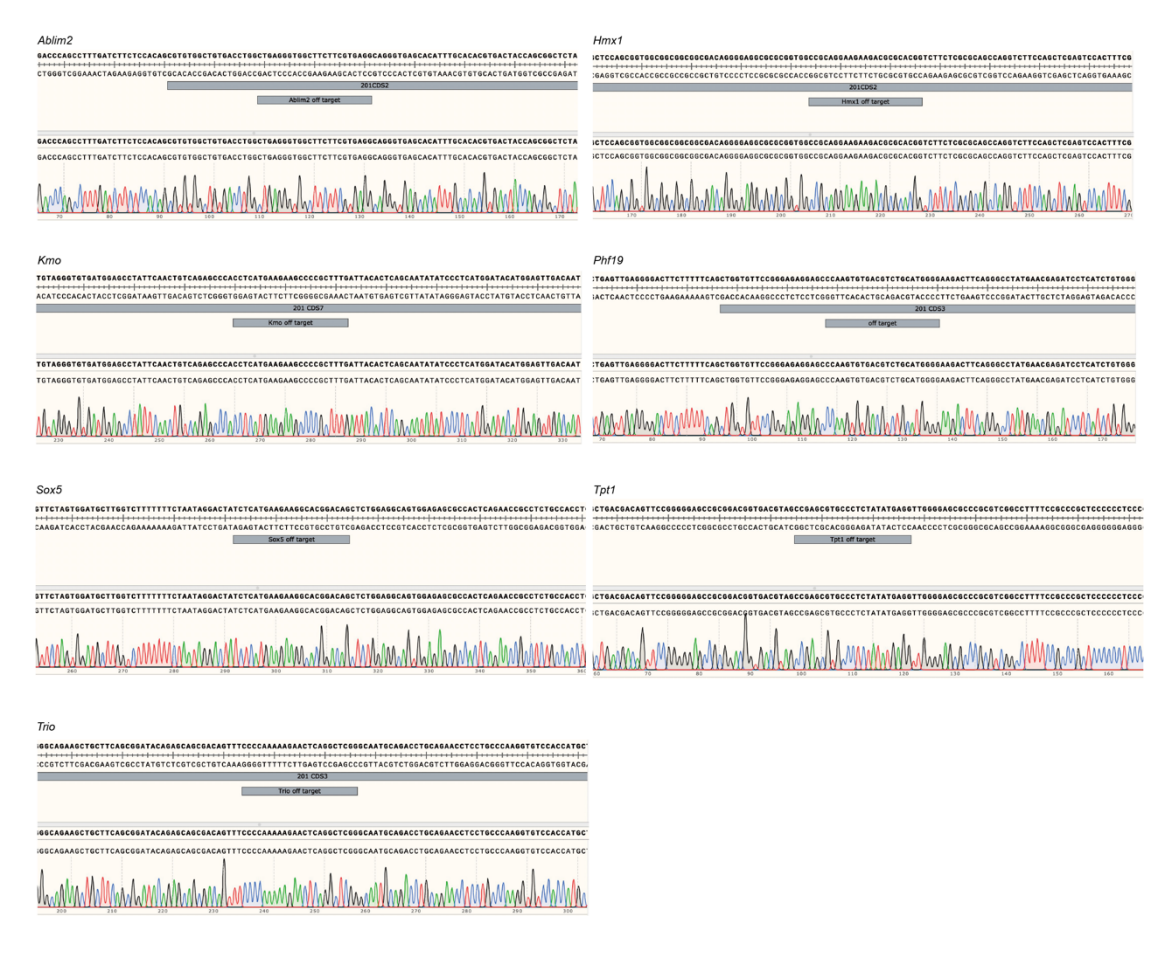
Supplementary Fig. 36 The correlation analysis between mouse body weight changes (a comparison of body weight between D0 and Dx, x = 2, 3, 4, 7) and metabolite levels (**a**: hepatic glucose; **b-c**: FFA). The mean body weight change was set as the dependent variable, the mean metabolite abundance as the fixed effect, and the genotype as a random effect.



Supplementary Fig. 37 Comparisons of haematocrit (HCT) measurements between $EPASI^{V162T/V162T}$ and $EPASI^{+/+}$ mouse individuals ($n = 12 \ vs \ 11 \ on \ D0, 6 \ vs \ 7 \ on \ D2,$ 7 $vs \ 12 \ on \ D3, 8 \ vs \ 9 \ on \ D4$ and 8 $vs \ 5 \ on \ D7$) under different treatments. The bars display mean \pm SD and two-sided t tests were applied. ns: no significant difference. P values for each group were 0.5205, 0.2704, 0.6692, 0.2004, and 0.8522. Source data are provided as a **Source Data** file.



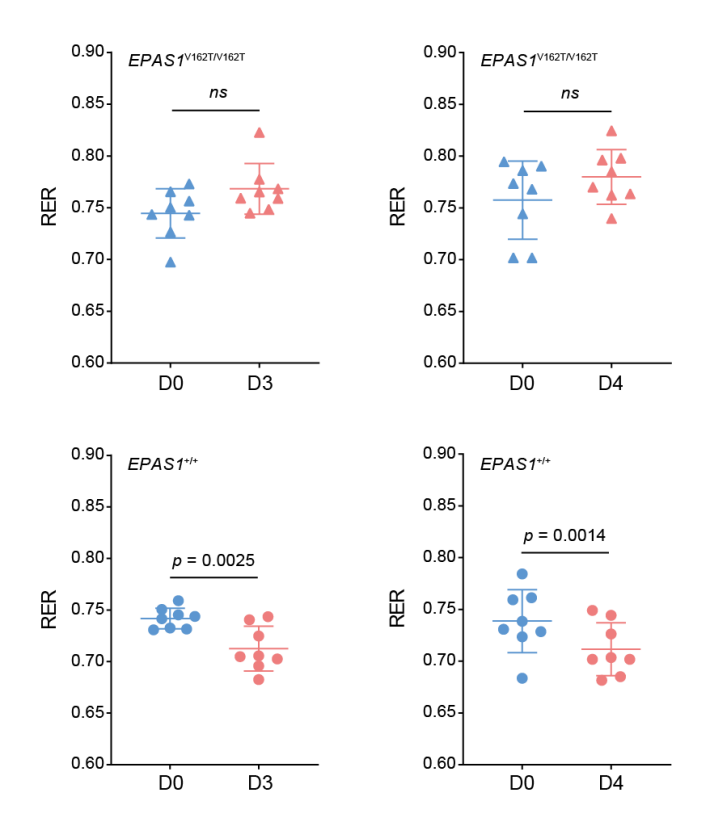
Supplementary Fig. 38 Comparison of survival time between $EPASI^{+/+}$ and $EPASI^{V162T/V162T}$ mouse individuals (n = 30 for each group) under acute hypoxia (4% O₂). The bars display mean \pm SD and a two-sided t test was applied. Source data are provided as a **Source Data** file.



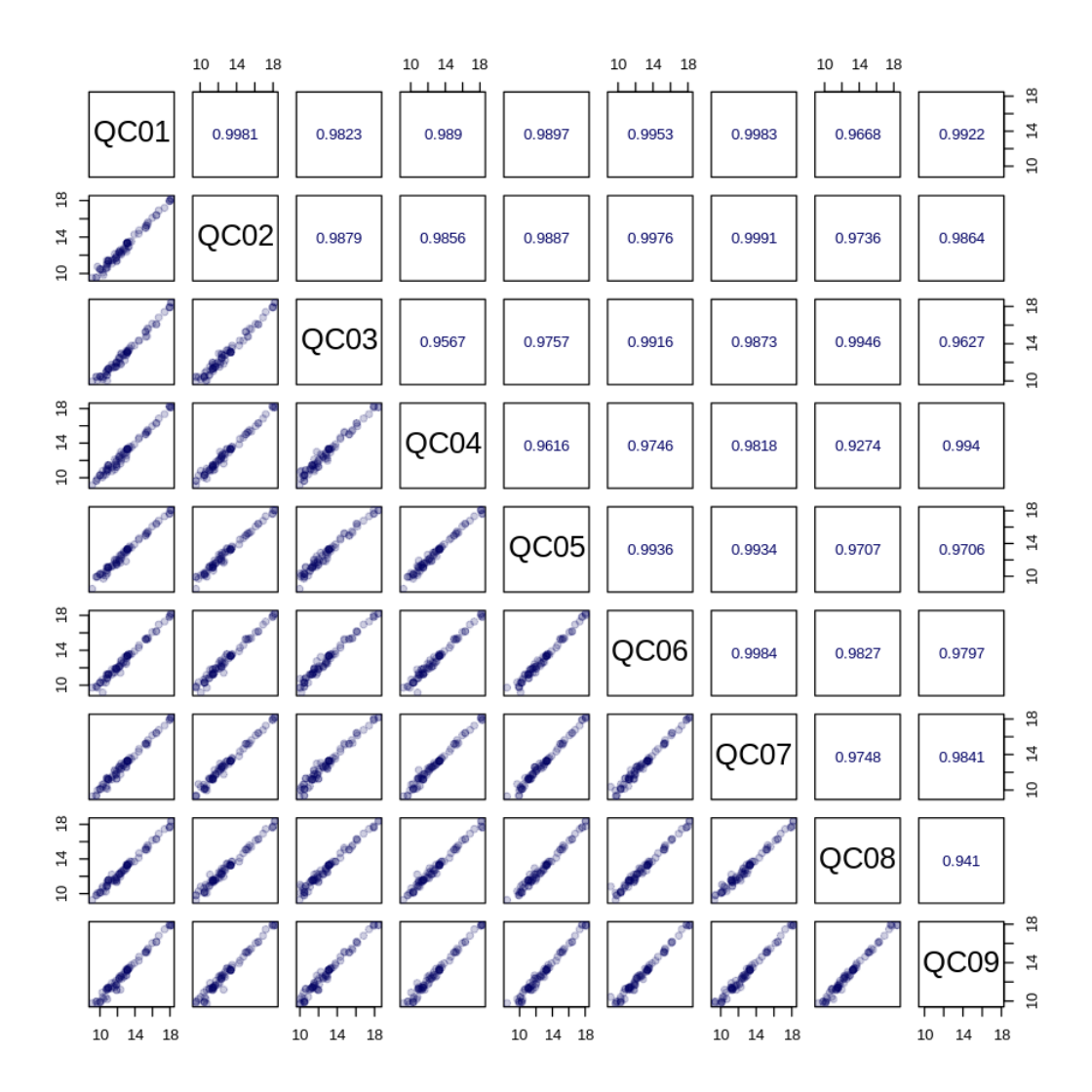
Supplementary Fig. 39 Sanger sequencing results of potential off-target genetic loci(exons).



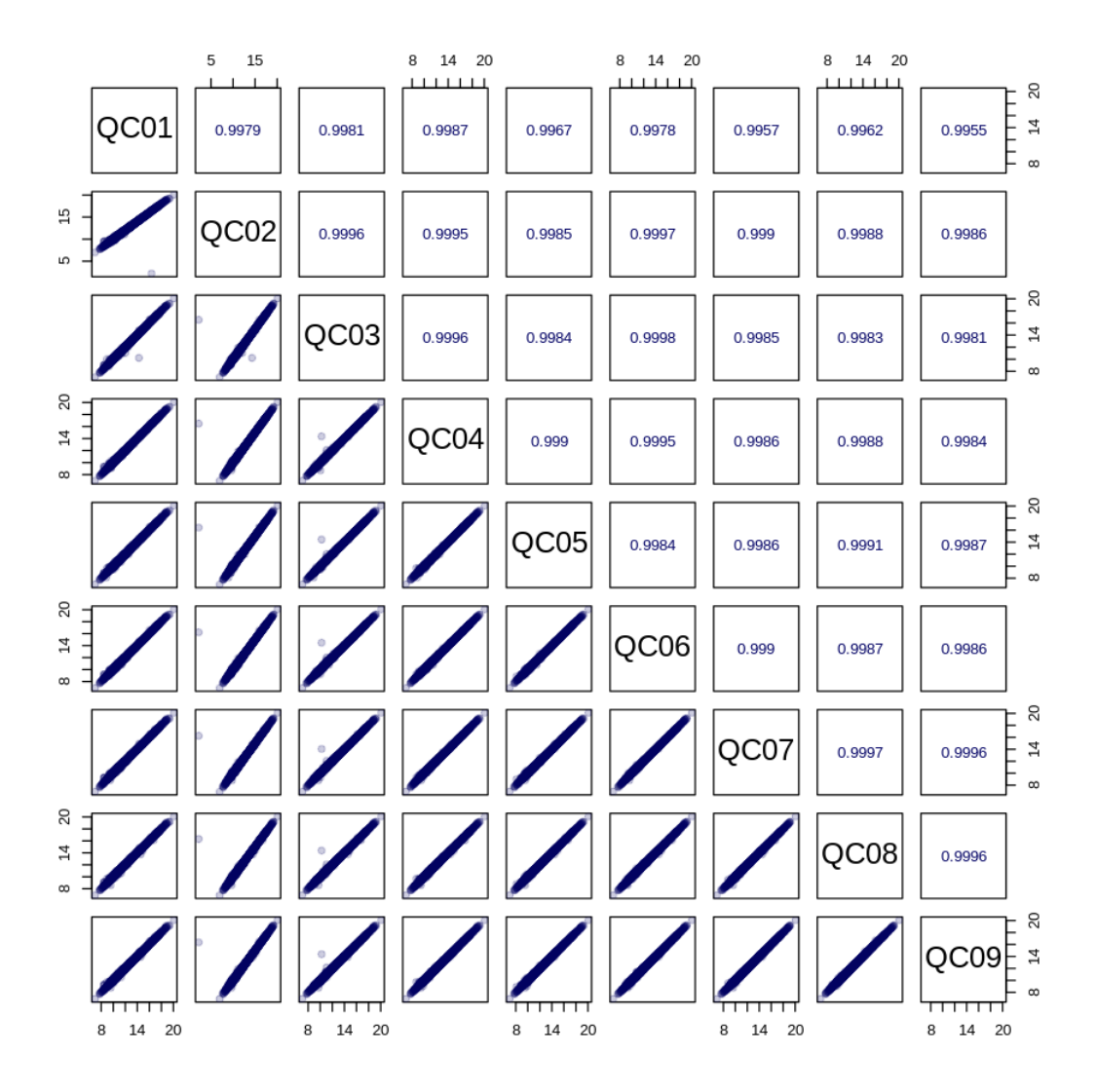
Supplementary Fig. 40 Sanger sequencing results of potential off-target genetic loci (introns).



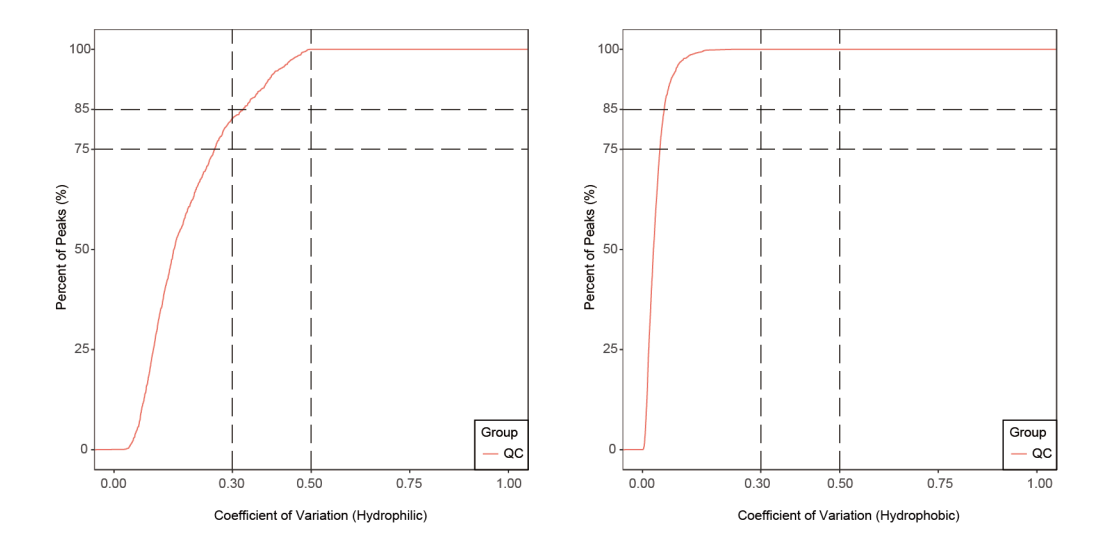
Supplementary Fig. 41 Measurements of respiratory exchange ratio (RER) in mutant (an additional independently derived knock-in mice) and wild type mice under hypoxia and normoxia (n = 8 for each group). The bars show mean \pm SD and two-sided t tests were applied. ns: no significant difference. P values were 0.1198 (D3 vs D0) and 0.2037 (D4 vs D0) in mutant mice. Source data are provided as a **Source**



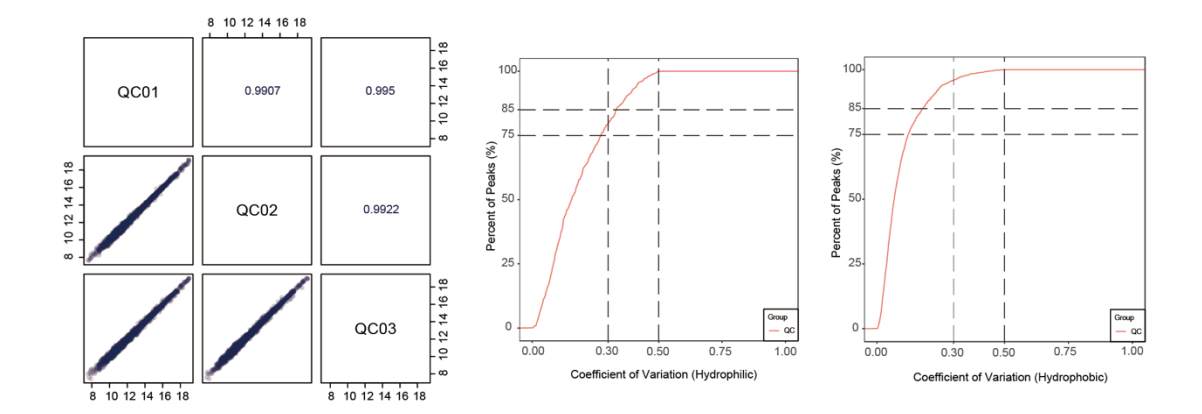
Supplementary Fig. 42 Pearson correlation plot of quality control (QC) samples used for hydrophilic metabolite detection in mouse livers. The diagonal squares represent the names of the QC samples for hydrophilic metabolite detection. The squares in the lower-left corner of the diagonal contain the corresponding scatter plots of the QC sample correlations, where the x and y axes represent the metabolite concentrations (Log-transformed). Each point in the plot represents a metabolite. The squares in the upper-right corner of the diagonal display the Pearson correlation coefficients for the corresponding QC samples.



Supplementary Fig. 43 Pearson correlation plot of QC samples used for hydrophobic metabolite detection in mouse livers. The diagonal squares represent the names of the QC samples for hydrophobic metabolite detection. The squares in the lower-left corner of the diagonal contain the corresponding scatter plots of the QC sample correlations, where the x and y axes represent the metabolite concentrations (Log-transformed). Each point in the plot represents a metabolite. The squares in the upper-right corner of the diagonal display the Pearson correlation coefficients for the corresponding QC samples.



Supplementary Fig. 44 Coefficient of variation (CV) distribution map of QC samples used for hydrophilic and hydrophobic extract detection in mouse livers. The x-axis represents the CV value, while the y-axis indicates the proportion of metabolites with a CV value lower than the corresponding value, relative to the total number of metabolites.



Supplementary Fig. 45 Pearson correlation plot (left) and CV distribution maps (middle and right) of QC samples used for hydrophilic and hydrophobic extract detection in plasmas of saker falcon. The diagonal squares represent the names of the QC samples for the detection. The squares in the lower-left corner of the diagonal contain the corresponding scatter plots of the QC sample correlations, where the x and y axes represent the metabolite concentrations (Log-transformed). Each point in the plot represents a metabolite. The squares in the upper-right corner of the diagonal display the Pearson correlation coefficients for the corresponding QC samples. In the CV distribution maps, the x-axis represents the CV value and the y-axis indicates the proportion of metabolites with a CV value lower than the corresponding value, relative to the total number of metabolites.

Supplementary Tables

261

262

Supplementary Table 1. Summary of glucose and lipid metabolic DEGs within the

same mouse type and DEGs between the two mouse types.

EPASI ^{V162T/V162T}	EPASI ^{+/+}	EPASI ^{V162T/V162T} vs EPASI ^{+/+}
<i>G6pc</i>	<i>G6pc</i>	<i>G6pc</i>
Gck	Gck	Gck
Hk3	Hk1/3	Hk3
Pygl	Pygl	
Gys2	Gys1/2	Gys2
Upg2		Upg2
		Gpi1
Pfkl	Pfkl	
Aldoa/c	Aldoc	Aldoa/b/c
Gapdh	Gapdh	
Pgam1/5	Pgam1/5	
Eno l	Eno1/3	Eno1
Pklr	Pklr	Pklr
Ldha/d	Ldha/b/d	Ldha
Pdha1	Pdha1	Pdha1
Pnpla2/3/6/7/8	Pnpla1/2/3/6/7/8	Pnpla1/2/7
Abhd2/5/11/15/18	Abhd2/4/6/8/10/11/13/15/18	Abhd2/4/6/8/11/13/15/18
Lipe	Lipe	
Plin2/4	Plin2/4/5	Plin2/3/4/5
	Mgll	Mgll
Cpt1a, Cpt2	Cptla	Cpt1a, Cpt2
Acsl1/4/5; Acsm1/2/3/5; Acsf2/3	Acsl1/3/4/5; Acsm1/2/5; Acsf2/3	Acsl1/3/4/5
Acad8/9/10/11/12; Acadsb	Acad8/9/10/11/12; Acadsb; Acads/m/l	Acad8/10/11/12; Acadm/l
Acaa1a/b; Acat1/2/3	Acaa1b; Acat2/3	Acaa1a/b; Acat3

Supplementary Table 2. Summary of explanatory degrees of different principal component analysis (PCA) components on behavioral parameters (breathing rate, food intake, food absorption, locomotion).

	PC1	PC2	PC3	PC4
Standard deviation	1.5186	1.0011	0.7826	0.2816
Proportion of variance	0.5765	0.2505	0.1531	0.0198
Cumulative proportion	0.5765	0.8271	0.9802	1.0000

Supplementary Table 3. Summary of the Vegf gene expression in falconized mice under hypoxia.

Gene ID	Full name	Up- or down-regulation	q value	Day
Vegfa	Vascular endothelial growth factor A	Down	2.24E-04	4
Vegfb	Vascular endothelial growth factor B	Down	2.28E-03	4

Supplementary Table 4. The qPCR primers for investigated candidate genes

involved in lipid metabolism.

Gene ID	Full name	Primer sequence (5' to 3')
ACSL1	Acyl-CoA synthetase	F: CTTTTGCAGCACTCACCACC
	long chain family	R: TCTTCGTGCACCACCACTAC
	member 1	
FASN	Fatty acid synthase	F: GTCTTGAACTCCTTGGCGGA
		R: AGGAAGATAGCCATGCCGAG
IDH1	Isocitrate dehydrogenase	F: AGGGTTGGCCTTTGTATCTG
	(NADP (+)) 1	R: CATGTCGTCGATGAGCCTATG
EPAS1	Endothelial PAS domain	F: CCTCCATCATGCGACTGGCAA
	protein 1	R: CACCACGGCAATGAAACCCTC
ACTB	Actin beta	F: GATGAGATTGGCATGGCTTT
		R: GTCACCTTCACCGTTCCAGT

Supplementary Table 5. The internal standards for hydrophilic compound detection
 in mouse liver tissues using UPLC-MS/MS.

Internal standard	Manufacture	Catalog No.	Concentration
Testosterone-[d3]	IsoReag	IR-15240S	1 μg/mL
Lidocaine	Dr. Ehrenstorfer	CDCT	1 μg/mL
L-2-chlorophenylalanine	J&K Scientific	106151-100mg	1 μg/mL
Sulfaquinoxaline-13C6	ANPEL	CDAA-540001-10mg	1 μg/mL
[2H5]-Phenoxy acetic Acid	IsoReag	IR-22227-250mg	1 μg/mL
L-Phenylalanine (2-13C, 99%)	TCI	ZTO-P0134-25g	1 μg/mL
succinic acid d4	Sigma	293075-5G	1 μg/mL

Supplementary Table 6. The internal standards for hydrophobic compound detection
 in mouse liver tissues using UPLC-MS/MS.

Internal standard	Manufacture	Catalog No.	Concentration
PC (13:0/13:0)	Avanti	850340P-25MG	0.5 μΜ
Cer (d18:1/4:0)	TRC	ZTR-C262550-50mg	0.2 μΜ
PE (12:0/12:0)	Cayman	15089	0.2 μΜ
PE (16:0-d31/18:1)	Avanti	860374P-10mg	0.2 μΜ
LPE (0:0/14:0)	Avanti	856735P-25mg	0.2 μΜ
2-Chloro-L-phenylalanine-1	J&K Scientific	106151-100mg	0.5 μΜ
PE (16:0_d31/18:1)	Avanti	860374P-10mg	0.2 μΜ
PC (13:0/13:0)	Avanti	850340P-25MG	0.5 μΜ

Supplementary Table 7. The external standards used for targeted metabolomics in mouse liver tissues.

External standard	Manufacture	Catalog No.	Concentration
Glucose	Sigma	158968-25g	0.1 μg/ml~150000 μg/ml
FFA (12:0)	Zzstandard	ZC-59052-100mg	0.01 μg/ml~50 μg/ml
FFA (18:3)	Zzstandard	ZC-59052-100mg	0.01 μg/ml~50 μg/ml

Supplementary Table 8. The internal standards for hydrophilic compound detection using UPLC-MS/MS for saker falcon plasma samples.

Internal standard	Manufacture	Catalog No.	Concentration
Sulfaquinoxaline-13C6	ANPEL	CDAA-540001-10mg	1 μg/mL
L-2-chlorophenylalanine	J&K Scientific	106151-100mg	1 μg/mL
4-Fluoro-L-α-phenylglycine	TCI	ZTO-F0862-1g	1 μg/mL
L-tryptophan-d5	Sigma	615862-500MG	1 μg/mL
[2H5]-Phenoxy acetic Acid	IsoReag	IR-22227-250mg	1 μg/mL
L-Phenylalanine (2-13C, 99%)	TCI	ZTO-P0134-25g	1 μg/mL
[2H5]-Hippuric Acid	TRC	ZTR-H356702-10mg	1 μg/mL

Supplementary Table 9. The internal standards for hydrophobic compound detection using UPLC-MS/MS for saker falcon plasma samples.

Internal standard	Manufacture	Catalog No.	Concentration
LPE (0:0/14:0)	Avanti	856735P-25mg	0.2 μΜ
CUDA	Zzstandard	ZC-23994-5mg	0.5 μΜ
PC (13:0/13:0)	Avanti	850340P-25MG	0.5 μΜ
PE (12:0/12:0)	Cayman	15089	0.2 μΜ
PE (16:0_d31/18:1)	Avanti	860374P-10mg	0.2 μΜ
PC (13:0/13:0)	Avanti	850340P-25MG	0.5 μΜ
PE (12:0/12:0)	Cayman	15089	0.2 μΜ
2-Chloro-L-phenylalanine-1	J&K Scientific	106151-100mg	0.5 μΜ